

AN ABSTRACT OF THE THESIS OF

GERALD BRUCE WEBB for the degree MASTER OF SCIENCE  
(Name of student) (Degree)

in Mechanical Engineering presented on May 9, 1975  
(Major Department) (Date)

Title: ANALYSIS OF AN EXTERNALLY LOADED PRESTRESSED

CYLINDRICAL SHELL

*O*  
*Redacted for Privacy*

Abstract approved:

*Hans J. Dahlke*

The concept of a prestressed cylindrical shell was investigated. In particular, a cylindrical shell constructed from coiled pressurized tubing was analyzed. This analysis was concentrated in two main areas, the first involved the failure modes of the prestressed cylinder. Both the buckling and yielding behavior of the tube walls was looked into. The second main area consisted of a comparison between conventional and prestressed cylinders of equal length, mean radius, and mass.

It appears from the theoretical analysis of a prestressed cylinder that the idea is indeed a workable one. It also appears that a prestressed cylinder is superior, in some instances, to a conventional cylinder, based on the comparisons that were made between the two.

**Analysis of an Externally Loaded  
Prestressed Cylindrical Shell**

**by**

**Gerald Bruce Webb**

**A THESIS**

**submitted to**

**Oregon State University**

**in partial fulfillment of  
the requirements for the  
degree of**

**Master of Science**

**June 1975**

APPROVED:

*Redacted for Privacy*

Associate Professor of Mechanical Engineering  
in charge of major

*Redacted for Privacy*

Head of Department of Mechanical Engineering

*✓*

*Redacted for Privacy*

Dean of Graduate School

Date thesis is presented May 9, 1975

Typed by Deanna L. Cramer for Gerald Bruce Webb

#### ACKNOWLEDGEMENTS

I wish to thank Dr. Hans Dahlke for the help and guidance he provided during the course of this project. I would also like to express my appreciation to my wife Elaine for the great patience she displayed, and the moral support she provided, during the writing of this thesis.

## TABLE OF CONTENTS

<u>Chapter</u>		<u>Page</u>
I	INTRODUCTION	1
II	ANALYSIS OF PRESTRESSED CYLINDRICAL SHELLS	7
III	RESULTS OF THE ANALYSIS OF A PRESTRESSED CYLINDRICAL SHELL	11
IV	ANALYSIS OF CONVENTIONAL CYLINDRICAL SHELLS	33
V	RESULTS OF THE ANALYSIS OF A CONVENTIONAL CYLINDRICAL SHELL	36
VI	COMPARISON OF RESULTS	39
VII	CONCLUSIONS	48
	BIBLIOGRAPHY	50
	APPENDICES	
	APPENDIX I. PRESTRESSED CYLINDRICAL SHELL ANALYSIS	52
	A. Buckling	52
	B. Yielding	61
	APPENDIX II. CONVENTIONAL CYLINDRICAL SHELL ANALYSIS	70
	A. Buckling	70
	B. Yielding	71
	APPENDIX III. COMPARISON OF CONVENTIONAL AND PRESTRESSED CYLINDRICAL SHELLS	73
	A. Prestressed Cylinder	73
	B. Conventional Cylinder	73

## LIST OF FIGURES

<u>Figure</u>		<u>Page</u>
1	"Cylinder within a cylinder"	3
2	Cylinder constructed from coiled tubing	4
3	Model of loaded tubing	8
4	Tube wall element	12
5	Model showing only contact forces and resulting moments	13
6	Plot of $P_t$ vs. $P_o$ for a prestressed cylinder	26
7	Plot of $P_o$ vs. $R/r$ for a prestressed cylinder with a tube wall thickness of 0.05 inches	29
8	Plot of $P_o$ vs. $R/r$ for a prestressed cylinder with a tube wall thickness of 0.30 inches	30
9	Plot of $P_o$ vs. $R/r$ for a prestressed cylinder with a tube wall thickness of 0.55 inches	31
10	Conventional cylinder	34
11	Plot of $P_o$ vs. $R/r$ for conventional and prestressed cylinders with a tube wall thickness of 0.05 inches	41
12	Plot of $P_o$ vs. $R/r$ for conventional and prestressed cylinders with a tube wall thickness of 0.30 inches	42
13	Plot of $P_o$ vs. $R/r$ for conventional and prestressed cylinders with a tube wall thickness of 0.55 inches	43
I-1	Model of loaded tubing	53
I-2	Tube wall element	54
I-3	Model showing only contact forces and resulting moments	58
II-1	Plot for determining number of lobes	71

LIST OF TABLES

<u>Table</u>		<u>Page</u>
III-1	Data for tube wall thickness of 0.05 inches	75
III-2	Data for tube wall thickness of 0.30 inches	76
III-3	Data for tube wall thickness of 0.55 inches	77

## LIST OF SYMBOLS

### Variables

P	Pressure (psi)
N	Distributed Normal Forces ( $\text{LB}_f/\text{in}$ )
M	Distributed Moments ( $\text{in-LB}_f/\text{in}$ )
V	Distributed Shear Forces ( $\text{LB}_f/\text{in}$ )
E	Modulus of Elasticity (psi)
$\nu$	Poisson's Ratio
t	Thickness (inches)
W	Radial Deflection (inches)
R	Mean Cylinder Radius (inches)
r	Mean Tube Radius (inches)

### Subscripts

o	Outside or External
i	Inside or Internal
t	Tube
r	Radial Direction
x	Longitudinal Direction
$\theta$	Circumferential Direction

ANALYSIS OF AN EXTERNALLY LOADED  
PRESTRESSED CYLINDRICAL SHELL

I. INTRODUCTION

The maximum uniform external loading that a cylindrical shell can be subjected to is determined by either buckling of the wall, or yielding of the wall material. Buckling and yielding are both a direct result of the compressive forces acting on the cylinder wall due to the external loading. If some method could be found to apply a tensile stress at the same time these compressive forces are acting, it should be possible to increase the maximum allowable external pressure (external loading) that the cylinder could withstand without failure by either buckling or yielding. Thus an externally loaded prestressed cylindrical shell is a shell acted on by external pressure, and at the same time is acted upon by tensile loadings introduced in some manner.

There are two possible methods of prestressing the walls of a cylindrical shell. The first method is to internally pressurize the cylinder. The second method is to pre-stress the cylinder wall in a manner that does not make use of internal pressurization. For this investigation the latter of the two methods listed above will be used. The main reason for this choice is the versatility that is possible. It is not always desirable (or possible) to subject the

inside of a cylinder to a pressure above a given level. For the first method the internal pressure varies directly with the desired maximum external pressure (for a cylinder of fixed size). By making use of the second method it may be possible to greatly reduce the required internal pressure, but still be able to withstand the desired external pressure. It also appears that for a given level of internal pressure a cylinder making use of the second method of pre-stressing could withstand a larger external pressure.

There seems to be two possible solutions to the problem of prestressing without internal pressurization. The first solution is to build what amounts to a "cylinder within a cylinder" as shown in Figure 1, and pressurize the space in between the walls. The second solution is to construct a cylinder from coiled tubing as shown in Figure 2, and pressurize the tubing. The second method of construction was chosen for analysis because it appears to be the easiest to actually construct, and it was felt that it was the best overall solution to the problem.

There are several reasons why the coiled tubing appears to be the best solution. The first, as stated previously is ease of construction. It would not take a great deal of expensive or complicated machinery to bend tubing made from most common structural materials into coils. This would probably be true up to fairly large sizes of tubing (up to quite large diameters). Even for large diameter tubing, the

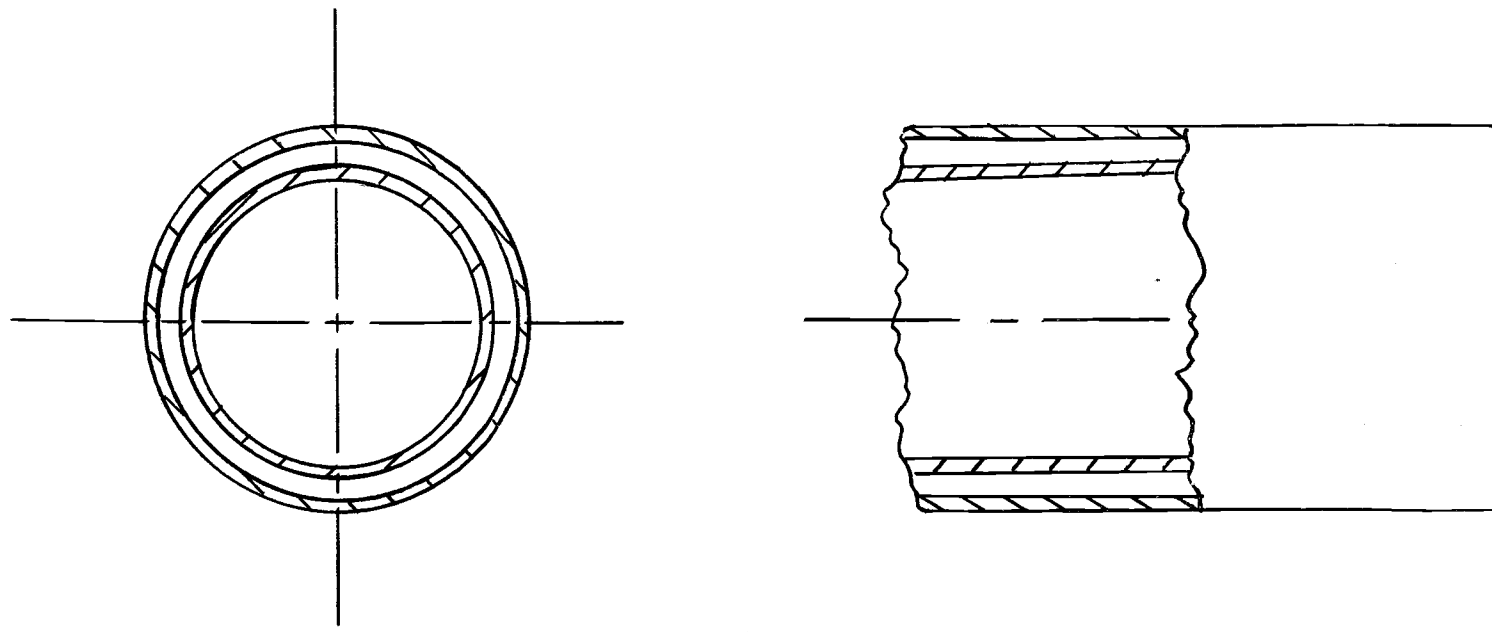


Figure 1. "Cylinder within a cylinder".

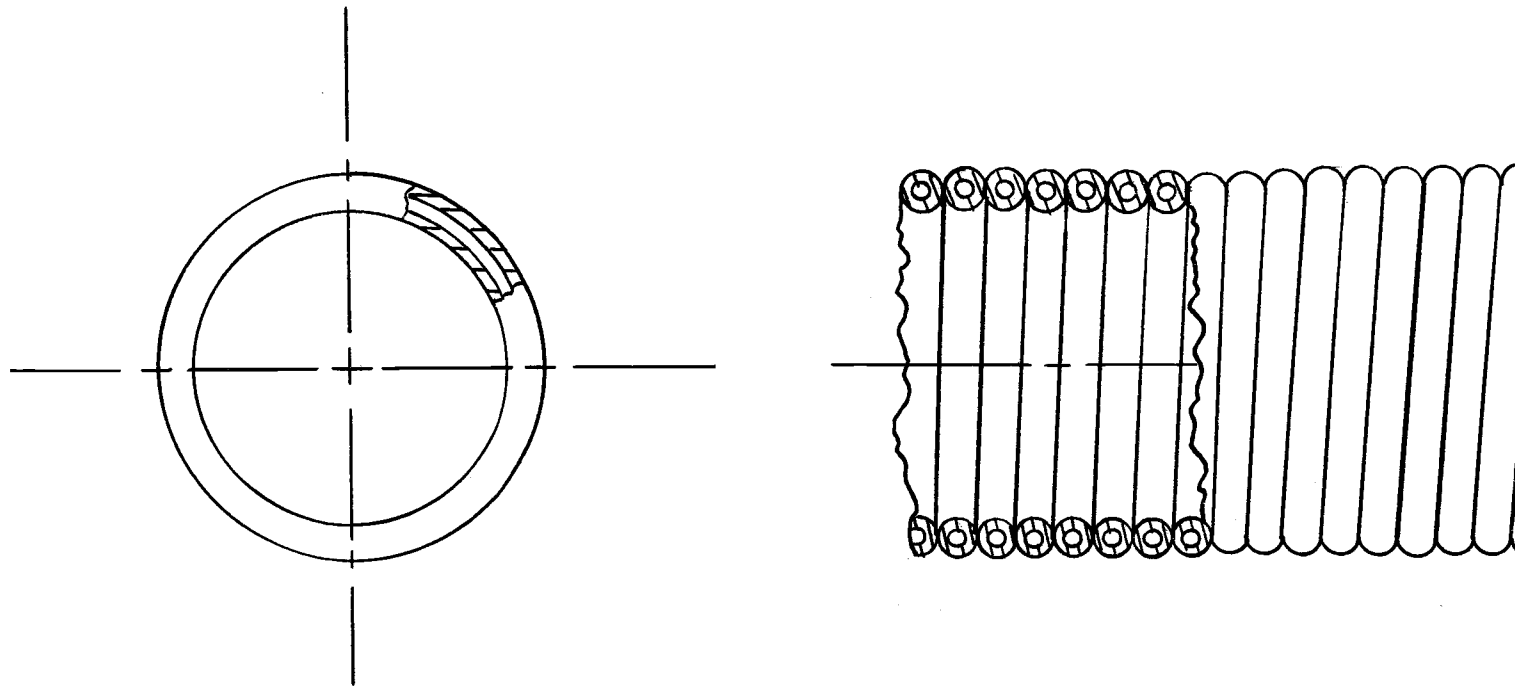


Figure 2. Cylinder constructed from coiled tubing.

time, effort and cost of bending the tubing into coils would probably not be prohibitive. The actual construction of the cylinder from this coiled tubing does not appear to be overly difficult either. It seems that it would be a fairly simple matter to continuously weld the adjacent coils of tubing together by rotating the whole cylinder, and moving it forward slowly so the cylinder is always in the proper position for welding.

The second reason has to do with pressurizing the tubing itself. Any substance (liquid or gas) could be used to pressurize the tubing provided it could meet any specifications which might be imposed on the system. This means that the tubing could possibly be used to store a liquid or a gas, while also using this substance as a means of pressurizing the tubing. So the tubing would serve a double role, to prestress the cylinder wall, and as a storage container.

Thus, it can be concluded that prestressing has definite advantages for use with externally loaded cylindrical shells. It also appears that the method of prestressing the cylinder walls without resorting to internal pressurization is the best method because of its versatility. It was decided to analyze a cylinder constructed from coiled tubing because of the apparent advantages of this method. The analysis will be purely theoretical in nature, and an attempt will be made to compare a prestressed cylindrical shell with a regular (or conventional) cylindrical shell.

The actual concept of prestressing a cylindrical shell by constructing it from coiled pressurized tubing was originated by Otto P. H. Dahlke in 1964, while employed by the Martin Company. He prepared a report entitled "Concept of a Prestressed Tubular Hull Structure" [7], in which he looked at the general feasibility of this method, along with obtaining general solutions for the system as a whole. In his report he also obtained solutions for the stress distribution in the tube wall due to the external pressure, but did not examine the buckling behavior. This project will represent an extension of his work, with the stress distributions looked at in a more detailed manner, and the buckling behavior of the tube walls examined in some detail.

## II. ANALYSIS OF PRESTRESSED CYLINDRICAL SHELLS

The analysis of a prestressed cylindrical shell constructed from coiled tubing is essentially an analysis of the behavior of the tubing itself, rather than the entire cylinder. For the investigation of a prestressed cylinder, several assumptions were made. The first assumption is that failure occurs when an element in the tube wall begins to yield. The second is that the tubing wall will either fail (buckle or yield) prior to failure of the cylinder, or at the same time as the cylinder fails. This appears to be a good assumption, because if the cylinder is to buckle, the tube walls must be plastically deformed, which is defined as failure. Also, the tubing must yield in order for the cylinder to yield, since the tubing makes up the cylinder wall. The third assumption is that the von Mises Yield Criterion (Distortion Energy Theory) adequately describes the stress state at any point in the tube wall. This failure theory was used because the relative magnitudes of the principal stresses were not known, and also because this theory has been shown to be the most accurate of the commonly used failure theories.

The tubing itself was modeled as shown in Figure 3. The two cross-sections A and B were chosen for analysis because the stresses are maximum at these points (i.e., the moment is at a maximum as well as the stress due to the

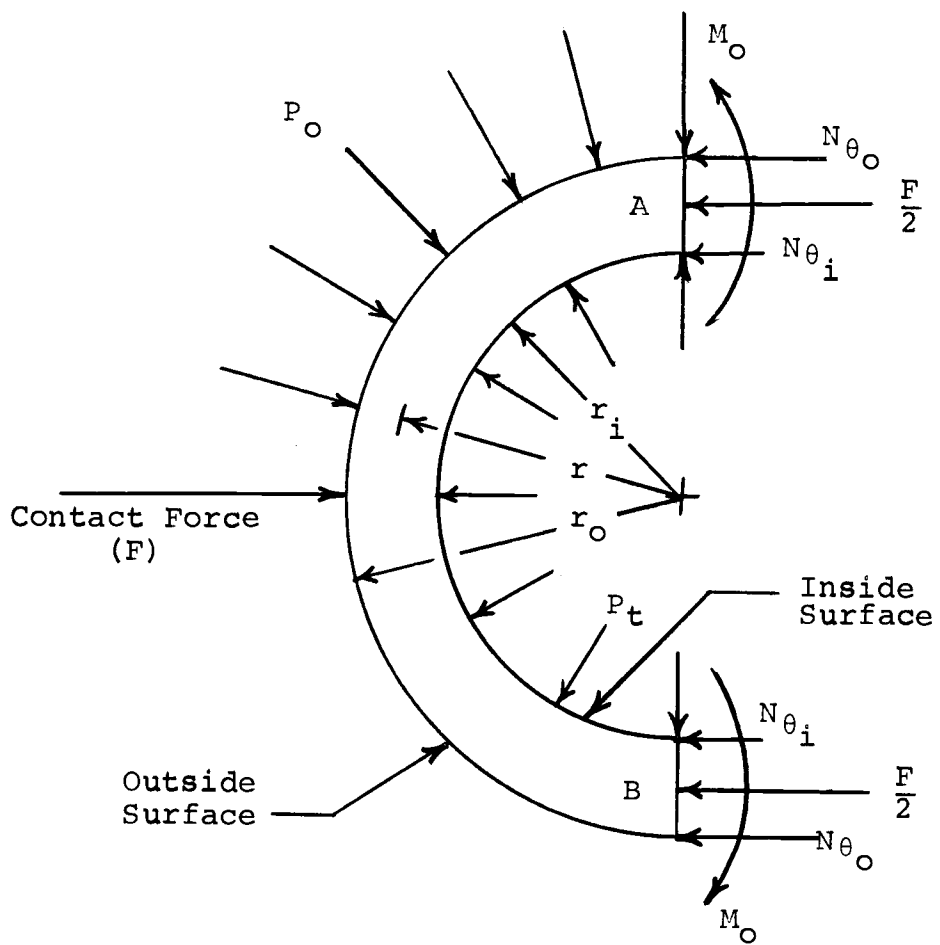


Figure 3. Model of loaded tubing.

contact force F). Analysis of the stress states will be done for the inside and outside tube surfaces at both cross-sections A and B because these two surfaces are the locations at which maximum stress levels occur. The tubing was considered to be simply supported at the two points of contact between adjacent tube sections. The prestressed cylinder itself was also considered to be simply supported, and perfectly rigid, in that no deflections or stresses result from its own weight.

For this investigation the tubing was assumed to be a thick-walled cylinder, which will make the analysis valid for any type of tubing (i.e., thin or thick-walled) because the thin-walled cylinder is merely a special case of the general thick-walled cylinder. Another assumption made was that the tubing was very long when compared to its diameter (essentially infinite in length). This seems to be a valid assumption, because for a cylinder of almost any size, the length of tubing required to construct it will be very much greater than the tubing diameter. As an example, for a cylinder ten inches in diameter, ten inches long, and constructed from tubing one-half inch in diameter, the length of tubing required would be approximately 630 inches, or a ratio of 1260:1 for tube length to tube diameter. For the actual analysis to be carried out, the tubing will be modeled as an infinitely long thick-walled cylinder subjected to the pressures, forces, and moments shown in Figure 3.

The actual analysis of the prestressed cylindrical shell involved calculations in two different areas. The first area was buckling of the tube wall when subjected to external pressure; and the second area was failure of the tube wall. As stated previously, failure and yielding of the wall material are considered to be synonymous.

### III. RESULTS OF THE ANALYSIS OF A PRESTRESSED CYLINDRICAL SHELL

The analysis of the buckling behavior of the tube wall was done by making use of the wall element shown in Figure 4. The displacement of the element was found by summing forces in the radial direction, and then letting the element shrink to an infinitesimal size (i.e., take limits as  $\Delta x$  and  $\Delta\theta$  go to zero). This results in a partial differential equation, which can be solved using the boundary conditions obtained by assuming the end of the tubing is simply supported (i.e., the end is pinned; and the deflection, moment and shear is zero). The equation thus obtained describes the radial deflection as a function of  $x$  and  $\theta$ . Due to the nature of the differential equation and the boundary conditions, all the integration constants cannot be solved for. For a complete analysis of the buckling behavior, the effects of the contact forces between adjacent sections of tubing must also be taken into consideration. The model used for the determination of the displacements caused by those forces can be seen in Figure 5. The total displacement of an element in the tube wall can now be found by superimposing these two solutions upon one another. The actual derivations, and calculations used to find the equation for the total radial displacement may be found in Appendix I, along with the equation for the displacement.

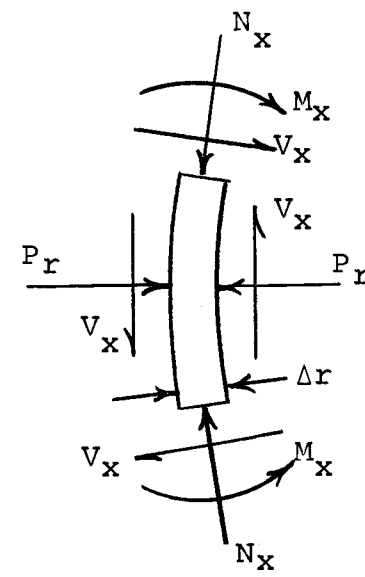
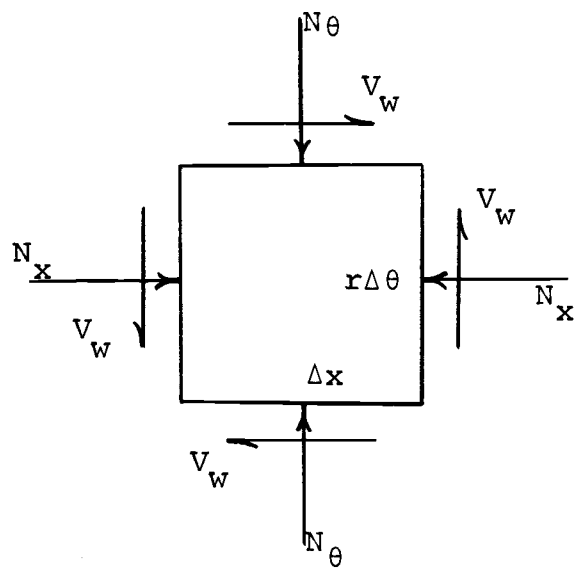
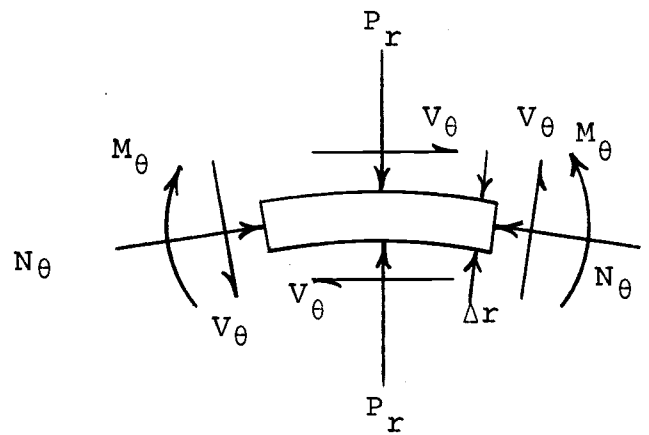


Figure 4. Tube wall element.

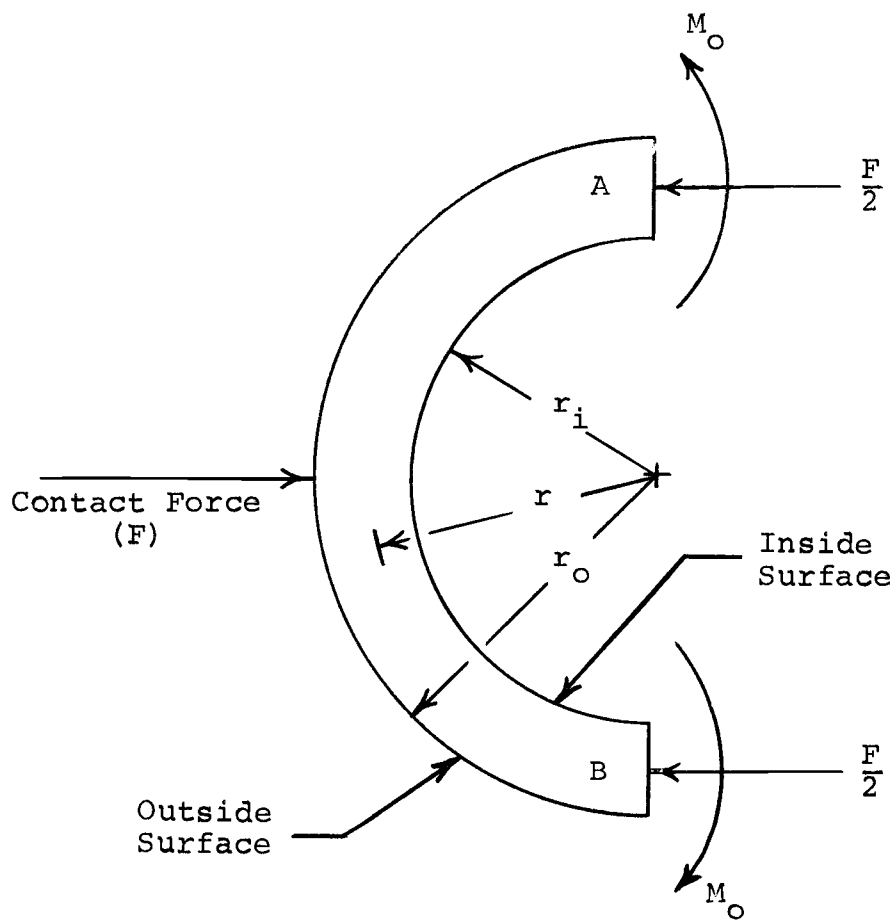


Figure 5. Model showing only contact forces and resulting moments.

Buckling of a plate or shell is defined to occur when the deflections of the plate or shell tend to increase without bound [14]. Using this definition we can find the critical loads at which buckling occurs. These are found by determining the values of longitudinal and circumferential loading at which the radial deflection tends to infinity. From these values the corresponding values of external pressure that cause buckling can be determined. The minimum of these values of external pressure is considered to be the critical value. Following this procedure, the critical load value is found to be

$$N_x = \pm \frac{Et^2}{r_i} \sqrt{\frac{t}{3(1 - \nu^2)}} \quad (1)$$

where  $N_x$  is the longitudinal force acting on the wall element. The corresponding value for the critical external pressure is

$$P_o = \frac{\pi}{\rho R_o} \left[ \frac{P_t r_i}{2} + Et(\rho - 1) \sqrt{\frac{t}{3(1 - \nu^2)}} \right] \quad (2)$$

where  $\rho = \frac{r_o}{r_i}$  and  $P_t$  is the internal tube pressure. An equation will be derived to determine the maximum value that  $P_t$  can assume, but the proper foundation for this derivation has not yet been laid, so it will be put off until a more appropriate time. A full derivation of Equations (1) and (2) may be found in Appendix I. It can be shown that the only possible solution for  $P_o$  is Equation (2), even

though the solution obtained using the quadratic equation shows that either a plus or minus sign may be used.

It can be seen from examination of Equation (1) that buckling of the tube wall is only a function of the longitudinal force, and is independent of the circumferential force. This result was not totally unexpected, because the buckling of an infinitely long flat strip is only a function of the longitudinal force acting upon it [14]. Since the tubing is similar in many ways to an infinitely long flat strip, due to the way in which it was modeled, the results should be similar. The critical load is also a function of the tube geometry (i.e., the tube and cylinder radii, and the tube wall thickness), and the material from which the tubing is made. This result also seems reasonable, because buckling of any body is dependent upon the geometry, and the material properties of that body [8, 14].

Examination of Equation (2) reveals that  $\underline{P}_O$  is a function of  $\underline{P}_t$  (the internal tube pressure), the cylinder and tube geometries, and the material properties. It can also be seen that the maximum allowable external pressure (i.e., the critical external pressure, or  $\underline{P}_O$ ) is a linear function of the internal tube pressure providing the material properties are constant, and the geometries remain fixed. The dependence of  $\underline{P}_O$  on  $\underline{P}_t$  is to be expected, because the resistance to buckling should increase as the internal tube pressure increases. This increase in resistance is a result of

the increase in tensile stresses in the tube wall caused by the increase in the internal tube pressure.

The failure analysis of the cylindrical shell was done by modeling the tubing as shown in Figures 4 and 5. The stresses due to the pressures acting on the tubing ( $P_o$  and  $P_t$ ) were determined by using the model of Figure 4. The stresses obtained by using the model of Figure 5 were then superimposed on the pressure induced stresses, with the final result being the total stress state for the tube wall.

As stated previously, the von Mises Yield Criterion will be used for the failure analysis. Using this criterion, and substituting expressions for the radial, circumferential, and longitudinal stresses, an equation can be derived involving both  $P_o$  and  $P_t$ . An expression for  $M_o$  can be derived in terms of the contact force between adjacent tube sections by making use of Castigliano's Theorems. If we assume  $P_t$  is a constant, the maximum value of  $P_o$  as a function of  $P_t$  can be solved for. This was done for the inside and outside tube surfaces at cross-sections A and B in Figure 3. The reasons for the use of these points have been previously stated in Section II. Actually going through the preceding analysis results in the following equations for  $P_o$

$$P_o = -\frac{B_i P_t}{2A_i} \pm \sqrt{\frac{B_i^2 P_t^2}{4A_i^2} + \frac{\sigma_y^2}{A_i} - \frac{C_i^2 P_t^2}{A_i}} \quad (3)$$

$$P_O = - \frac{B_O P_t}{2A_O} \pm \sqrt{\frac{B_O^2 P_t^2}{4A_O^2} + \frac{\sigma_y^2}{A_O} - \frac{C_O P_t^2}{A_O}} \quad (4)$$

$$P_O = - \frac{\beta_i P_t}{2\gamma_i} \pm \sqrt{\frac{\beta_i^2 P_t^2}{4\gamma_i^2} + \frac{\sigma_y^2}{\gamma_i} - \frac{\alpha_i P_t^2}{\gamma_i}} \quad (5)$$

$$P_O = - \frac{\beta_o P_t}{2\gamma_o} \pm \sqrt{\frac{\beta_o^2 P_t^2}{4\gamma_o^2} + \frac{\sigma_y^2}{\gamma_o} - \frac{\alpha_o P_t^2}{\gamma_o}} \quad (6)$$

where

$$\begin{aligned} A_i &= \frac{\rho R_o}{\pi t} \left[ \frac{\rho R_o}{\pi t} - \frac{2\rho^2}{\rho^2 - 1} - \frac{\phi}{2t} + \frac{3\phi r}{t^2} \left( \frac{2}{\pi} - 1 \right) \right] \\ &\quad + \left[ \frac{2\rho^2}{\rho^2 - 1} + \frac{\phi}{2t} - \frac{3\phi r}{t^2} \left( \frac{2}{\pi} - 1 \right) \right]^2 \end{aligned}$$

$$\begin{aligned} B_i &= \frac{\rho R_o}{\pi t} \left[ \frac{1}{\rho - 1} + \frac{\rho^2 + 1}{\rho^2 - 1} - 1 \right] \\ &\quad + \left[ \frac{1}{2(\rho - 1)} - \frac{2(\rho^2 + 1)}{\rho^2 - 1} + 1 \right] \left[ \frac{2\rho^2}{\rho^2 - 1} + \frac{\phi}{2t} \right. \\ &\quad \left. - \frac{3\phi r}{t^2} \left( \frac{2}{\pi} - 1 \right) \right] \end{aligned}$$

$$\begin{aligned} C_i &= \left[ \frac{\rho^2 + 1}{\rho^2 - 1} \right] \left[ \frac{\rho^2 + 1}{\rho^2 - 1} - \frac{1}{(\rho - 1)} + 1 \right] \\ &\quad + \left[ \frac{1}{4(\rho - 1)^2} + \frac{1}{2(\rho - 1)} + 1 \right] \end{aligned}$$

$$\begin{aligned}
A_O &= \frac{\rho R_O}{\pi t} \left[ \frac{\rho R_O}{\pi t} - \frac{\rho^2 + 1}{\rho^2 - 1} - \frac{\theta}{2t} - \frac{3\theta r}{t^2} \left( \frac{2}{\pi} - 1 \right) \right] \\
&\quad + \left[ \frac{\rho^2 + 1}{\rho^2 - 1} + \frac{\theta}{2t} + \frac{3\theta r}{t^2} \left( \frac{2}{\pi} - 1 \right) \right]^2 - \left[ \frac{\rho^2 + 1}{\rho^2 - 1} \right] \\
&\quad - \frac{\theta}{2t} - \frac{3\theta r}{t^2} \left( \frac{2}{\pi} - 1 \right) + 1 \\
B_O &= \frac{\rho R_O}{\pi t} \left[ \frac{2}{\rho^2 - 1} - \frac{1}{\rho - 1} \right] + \left[ \frac{\rho^2 + 1}{\rho^2 - 1} \right] \left[ \frac{1}{2(\rho - 1)} \right. \\
&\quad \left. - \frac{4}{\rho^2 - 1} \right] + \left[ \frac{1}{2(\rho - 1)} - \frac{4}{\rho^2 - 1} \right] \left[ \frac{\theta}{2t} \right. \\
&\quad \left. + \frac{3\theta r}{t^2} \left( \frac{2}{\pi} - 1 \right) \right] + \frac{2}{\rho^2 - 1} + \frac{1}{2(\rho - 1)} \\
C_O &= \left[ \frac{1}{\rho^2 - 1} \right] \left[ \frac{4}{\rho^2 - 1} - \frac{1}{\rho - 1} \right] + \frac{1}{4(\rho - 1)^2} \\
\alpha_i &= C_i \\
\beta_i &= \left[ \frac{1}{2(\rho - 1)} - \frac{2(\rho^2 + 1)}{\rho^2 - 1} - 1 \right] \left[ \frac{\theta}{2t} - \frac{3\theta r}{t^2} \left( \frac{2}{\pi} - 1 \right) \right] \\
&\quad + \frac{\rho R_O}{\pi t} \left[ \frac{\rho^2 + 1}{\rho^2 - 1} - \frac{1}{\rho - 1} - 1 \right] \\
\gamma_i &= \left[ \frac{\rho R_O}{\pi t} - \frac{\theta}{2t} + \frac{3\theta r}{t^2} \left( \frac{2}{\pi} - 1 \right) \right]^2 \\
&\quad + \frac{\rho R_O}{\pi t} \left[ \frac{\theta}{2t} - \frac{3\theta r}{t^2} \left( \frac{2}{\pi} - 1 \right) \right] \\
\alpha_o &= C_o
\end{aligned}$$

$$\beta_o = \left[ \frac{1}{2(\rho - 1)} - \frac{2}{\rho^2 - 1} \right] \left[ \frac{\vartheta}{2t} + \frac{3\vartheta r}{t^2} \left( \frac{2}{\pi} - 1 \right) \right]$$

$$+ \frac{\rho R_o}{\pi t} \left[ \frac{2}{\rho^2 - 1} - \frac{1}{\rho - 1} \right]$$

$$\gamma_o = \left[ \frac{\rho R_o}{\pi t} - \frac{\vartheta}{2t} - \frac{3\vartheta r}{t^2} \left( \frac{2}{\pi} - 1 \right) \right]^2$$

$$+ \frac{\rho R_o}{\pi t} \left[ \frac{\vartheta}{2t} + \frac{3\vartheta r}{t^2} \left( \frac{2}{\pi} - 1 \right) \right]$$

$$\rho = \frac{r_o}{r_i}$$

$$r = \frac{r_o + r_i}{2}$$

$$\sigma_y = \text{yield stress}$$

The quantity  $\vartheta$  is some loading function that relates the contact force  $F$ , and the external pressure  $P_o$  such that

$$F = \vartheta P_o$$

where  $\vartheta$  is defined to be positive if the force  $F$  is as shown in Figure 3, and negative if  $F$  is opposite that shown in Figure 3. For the case of external hydrostatic pressure,

$$\vartheta = \frac{R_o^2}{2R}$$

where  $R$  is the mean cylinder radius (the radius measured from the center of the cylinder to the center of the tubing), and  $R_o$  is the outside cylinder radius such that

$$R_o = R + r_o$$

The actual derivation of Equations (3), (4), (5), and (6) may be found in Appendix I. The sign that is used in each of Equations (3) through (6) is the one that results in the minimum value of  $P_o$ . A negative value for  $P_o$  is considered to be undefined.

The maximum external pressure allowed from the viewpoint of yielding is found in the following manner. For a given geometrical arrangement of cylinder and tubing, and a given internal tube pressure ( $P_t$ ) the external pressure is calculated from each of Equations (3) through (6). Once this has been done, the four values of  $P_o$  are compared, with the minimum one being considered the maximum allowable external pressure. The calculated value of  $P_o$  is the value at which yielding first begins at a point on the tube wall, and by definition this is when failure occurs. Since all four values obtained for  $P_o$  define failure at different points on the tube wall, the minimum of these four points must be used as the critical value of  $P_o$  (i.e., the value at which yielding first occurs).

To determine the maximum value of the external pressure for a given value of internal tube pressure, both buckling and failure must be considered. The minimum of the two values obtained for the critical external pressure

from these two considerations is considered to be the overall critical value of the external pressure.

The previous analysis of failure of the tubing due to yielding has laid the groundwork for determining the maximum allowable internal tube pressure. As before, the von Mises Yield Criterion will be used. If we assume that  $\underline{P}_C$  is a constant (or a fixed value) then  $\underline{P}_t$  can be solved for, using the same method that we used previously to solve for  $\underline{P}_o$ . Following this procedure results in four equations expressing  $\underline{P}_t$  as a function of  $\underline{P}_o$ , the material yield strength, and the geometry of the tube and cylinder. These four equations are

$$\underline{P}_t = - \frac{B_i P_o}{2C_i} \pm \sqrt{\frac{B_i^2 P_o^2}{4C_i^2} + \frac{\sigma_y^2}{C_i} - \frac{A_i P_o^2}{C_i}} \quad (7)$$

$$\underline{P}_t = - \frac{B_o P_o}{2C_o} \pm \sqrt{\frac{B_o^2 P_o^2}{4C_o^2} + \frac{\sigma_y^2}{C_o} - \frac{A_o P_o^2}{C_o}} \quad (8)$$

$$\underline{P}_t = - \frac{\beta_i P_o}{2\alpha_i} \pm \sqrt{\frac{\beta_i^2 P_o^2}{4\alpha_i^2} + \frac{\sigma_y^2}{\alpha_i} - \frac{\gamma_i P_o^2}{\alpha_i}} \quad (9)$$

$$\underline{P}_t = - \frac{\beta_o P_o}{2\alpha_o} \pm \sqrt{\frac{\beta_o^2 P_o^2}{4\alpha_o^2} + \frac{\sigma_y^2}{\alpha_o} - \frac{\gamma_o P_o^2}{\alpha_o}} \quad (10)$$

where all terms are the same as those previously defined.

It is obvious from Equations (7) through (10) that two solutions may actually exist for the value of the internal tube pressure. If the value calculated for  $\underline{P}_t$  using the minus sign is less than zero (negative), the only possible

solution is the equation with a plus sign. If the values of  $P_t$  calculated using both the plus and the minus signs are positive, the minimum of these two values is the proper one to use.

Two different methods may be used to determine the maximum allowable tube pressure. The first method involves incrementing the external pressure ( $P_o$ ). This is done by assuming an initial value for  $P_o$  of zero. The external pressure is then increased until a limiting value is reached. This value is determined when either the quantity under the square root sign in Equations (7) through (10) becomes negative, or when the value of  $P_t$  itself becomes negative. The maximum value of  $P_t$  calculated during this process (the incrementing of  $P_o$ ) is then considered to be the maximum allowable internal tube pressure. This process must be repeated for each of Equations (7) through (10), with the smallest value of the four maximum values being used for the maximum value of  $P_t$  (i.e., the minimum of the four values is to be used). Using this process the maximum value of  $P_t$  can be determined to any accuracy desired.

The second method for obtaining the maximum value of  $P_t$  is to differentiate the four expressions for the internal tube pressure [Equations (7) through (10)] with respect to  $P_o$ . The differential is then set equal to zero, and the resulting equations solved. The four equations obtained by following this procedure are

$$P_o = \frac{\sigma_y}{\left[ \frac{4C_i A_i^2}{B_i^2} - A_i \right]^{\frac{1}{2}}} \quad (11)$$

$$P_o = \frac{\sigma_y}{\left[ \frac{4C_o A_o^2}{B_o^2} - A_o \right]^{\frac{1}{2}}} \quad (12)$$

$$P_o = \frac{\sigma_y}{\left[ \frac{4\alpha_i \gamma_i^2}{\beta_i^2} - \gamma_i \right]^{\frac{1}{2}}} \quad (13)$$

$$P_o = \frac{\sigma_y}{\left[ \frac{4\alpha_o \gamma_o^2}{\beta_o^2} - \gamma_o \right]^{\frac{1}{2}}} \quad (14)$$

These four equations result in the values of  $P_o$  at which the maximum value of  $P_t$  may occur. To find this possible maximum, substitute the values obtained for  $P_o$  into the corresponding equations for  $P_t$  (i.e., substitute the value from Equation (12) into Equation (7), that from Equation (13) into Equation (8), etc.). The smallest of the four values obtained for  $P_t$  in this manner is considered to be the maximum value of  $P_t$ . The preceding method will not give the true maximum allowable tube pressure in all cases, but it should be used first, because it is much simpler and quicker than the iterative process. A quick check to determine if in fact the calculated value is the true maximum is to take an external pressure somewhat above the calculated value, and one somewhat below, and

substitute these into the equation that resulted in the value used for the maximum  $P_t$ . The iterative process must be used if either of these two new values results in a value of  $P_t$  greater than the assumed maximum.

This second method is really only a special case, with the first method of solution being the most general method. The iterative process applies to all cases, including those to which Equations (11) through (14) apply, and is very well suited to computerized analysis. It should also be noted that the maximum value of the external pressure does not necessarily occur at the maximum internal tube pressure, as will later be shown.

The first step in the determination of the maximum allowable external pressure is an iteration process similar to that used in the determination of the maximum tube pressure. Values of  $P_o$  are calculated from Equations (3) through (6). The value of  $P_t$  is allowed to vary from zero to the maximum value of  $P_t$  calculated by the method described previously. The values of  $P_o$  from buckling considerations [Equation (2)] are also calculated. One of several different methods of analysis must now be followed, dependent on the values of  $P_o$  calculated.

An example of the most general case may be found in Figure 6. It can be seen from this graph that the five plots of  $P_o$  versus  $P_t$  intersect at different points (such as point A). These points of intersection may be determined

in a purely graphical manner by making a very accurate plot, and reading the values for the points of intersection directly from it. The points may also be determined by a combination graphical-analytical method. The approximate intersection point is determined from the graph, and then iterations are performed around this point to determine the exact value. A third approach to determining the points of intersection is a purely analytical one. The points of intersection can be determined by comparison of the calculated values of  $P_o$  obtained from the five different equations by comparing them two at a time. If the value of  $P_o$  from one equation (say  $P_{o1}$ ) is greater than the value from the second equation ( $P_{o2}$ ) at a given  $P_t$ , and the reverse is true at some higher value of  $P_t$  (i.e.,  $P_{o2}$  is now greater than  $P_{o1}$ ), then the two equations have intersected at some point between these two values of  $P_t$ . The exact value of this intersection point may be determined by iterating between these values of  $P_t$ .

The reason for determining the points of intersection for the five plots of external pressure versus tube pressure has to do with finding the maximum allowable value for the external pressure. The maximum value of  $P_o$  at a given tube pressure is the minimum of the five values calculated using Equations (2) through (6). Using the preceding definition for the maximum value of  $P_o$ , and using the plots shown in Figure 6, it can be seen that the overall maximum value for

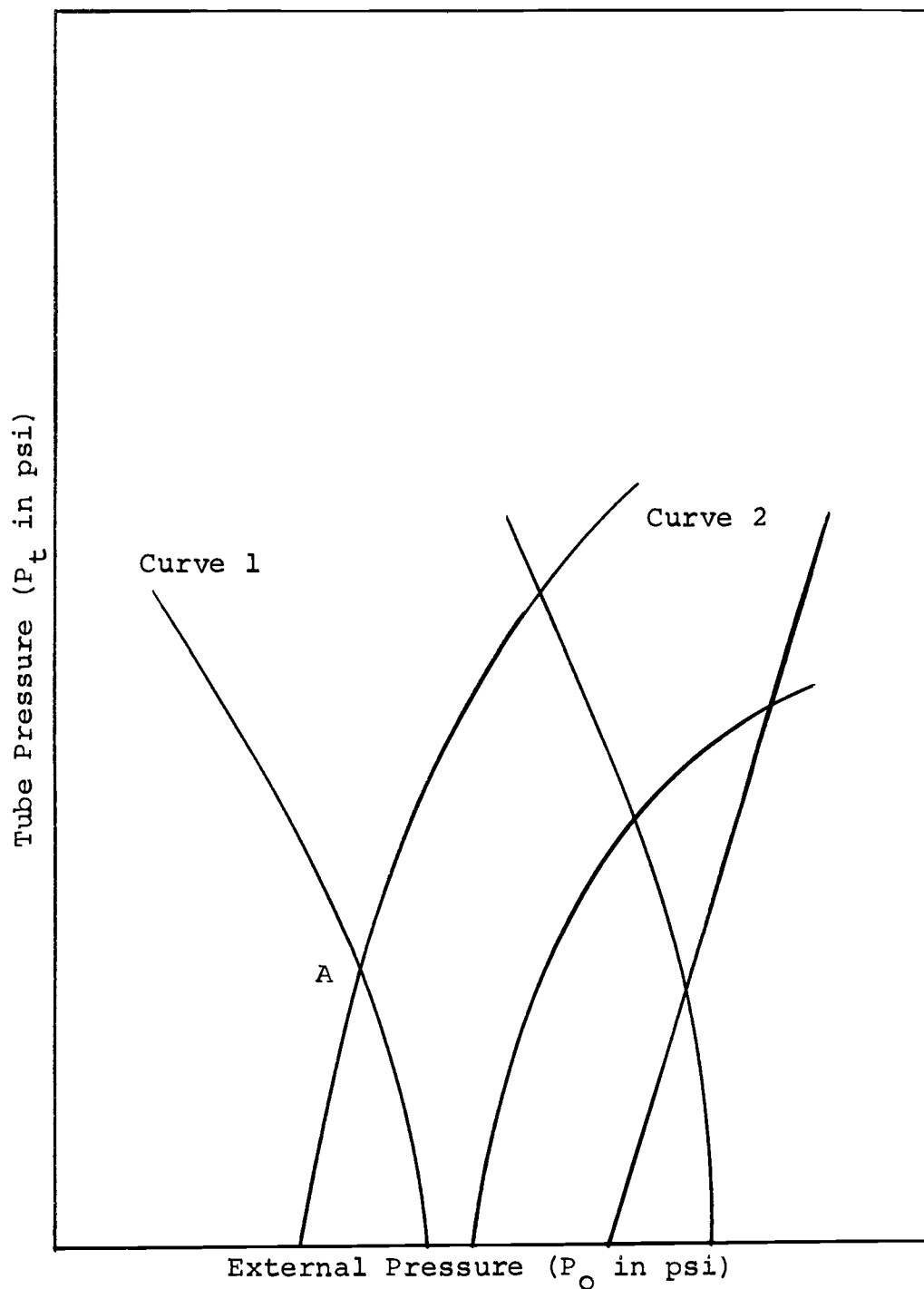


Figure 6. Plot of  $P_t$  vs.  $P_o$  for a prestressed cylinder.

$P_o$  occurs at point A, where curves (1) and (2) intersect. This preceding example points up the fact that if two different curves of  $P_o$  versus  $P_t$  intersect, the maximum allowable value of external pressure will occur at the point of intersection.

If some or all of the curves do not intersect one another, a different procedure for determining the maximum value of  $P_o$  must be followed. If one of the non-intersecting curves lies entirely to the left of the other four, the determination of  $P_o$  is based on it alone. For this case the maximum value of  $P_o$  from the curve is considered to be the critical value of external pressure. If all of the non-intersecting curves lie entirely to the right of a pair of curves that intersect, the point of intersection is the maximum value of  $P_o$ , just as for the case where all curves intersect one another. If a curve is intersected by more than one other curve, the point of intersection which results in the smallest value for external pressure is used. The value of tube pressure that results in the maximum efficiency of the prestressing system is that value which corresponds to the maximum allowable external pressure for the given system.

There are several interesting conclusions that can be drawn from the plots shown in Figures 7 through 9. The first thing immediately noticeable is that the maximum allowable pressure ( $P_o$ ) decreases as a function of mean

cylinder radius ( $R$ ) for a given ratio of mean cylinder radius to mean tube radius ( $R/r$ ). Closer examination of these curves also reveals that the required tube radius varies as a function of  $R$  for a given value of  $P_0$ . In fact, the required tube radius decreases as the cylinder radius increases. It can also be seen that the maximum external pressure allowed increases as  $R/r$  gets larger. This means that the cylinder in essence becomes stronger as the tube size decreases. This probably occurs because the surface area of the tube exposed to external pressure decreases as the tube radius decreases. This results in a diminished state of stress in the tube wall, and hence the strengthening effect as the tube size decreases. It can also be seen that the plot for a mean cylinder radius of 50 inches is not a straight line as are the plots for the other three radii. This applies in a varying degree to each of Figures 7 through 9. The reasons for this non-linearity are not known at this time, but it apparently has something to do with the relationship between the cylinder radius, and the external pressure. It should be noted that in plotting the curves shown in Figures 7 through 9 that a logarithmic scale was used on both the horizontal and vertical axes, and the length of the cylinder was assumed to be equal to its radius for calculation purposes.

It appears from looking at Figures 8 and 9 that there is a point at which maximum benefit is derived from the

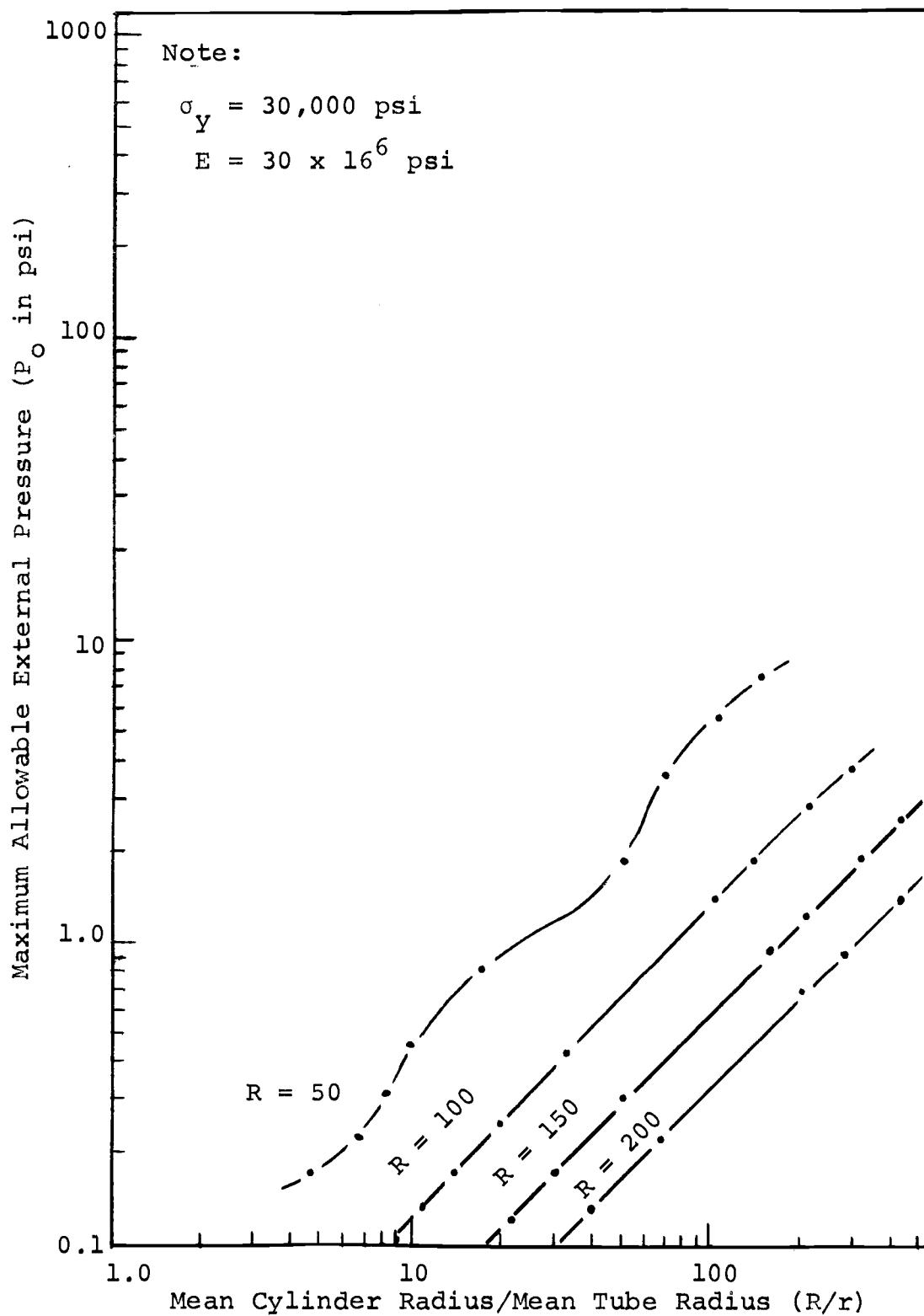


Figure 7. Plot of  $P_o$  vs.  $R/r$  for a prestressed cylinder with a tube wall thickness of 0.05 inches.

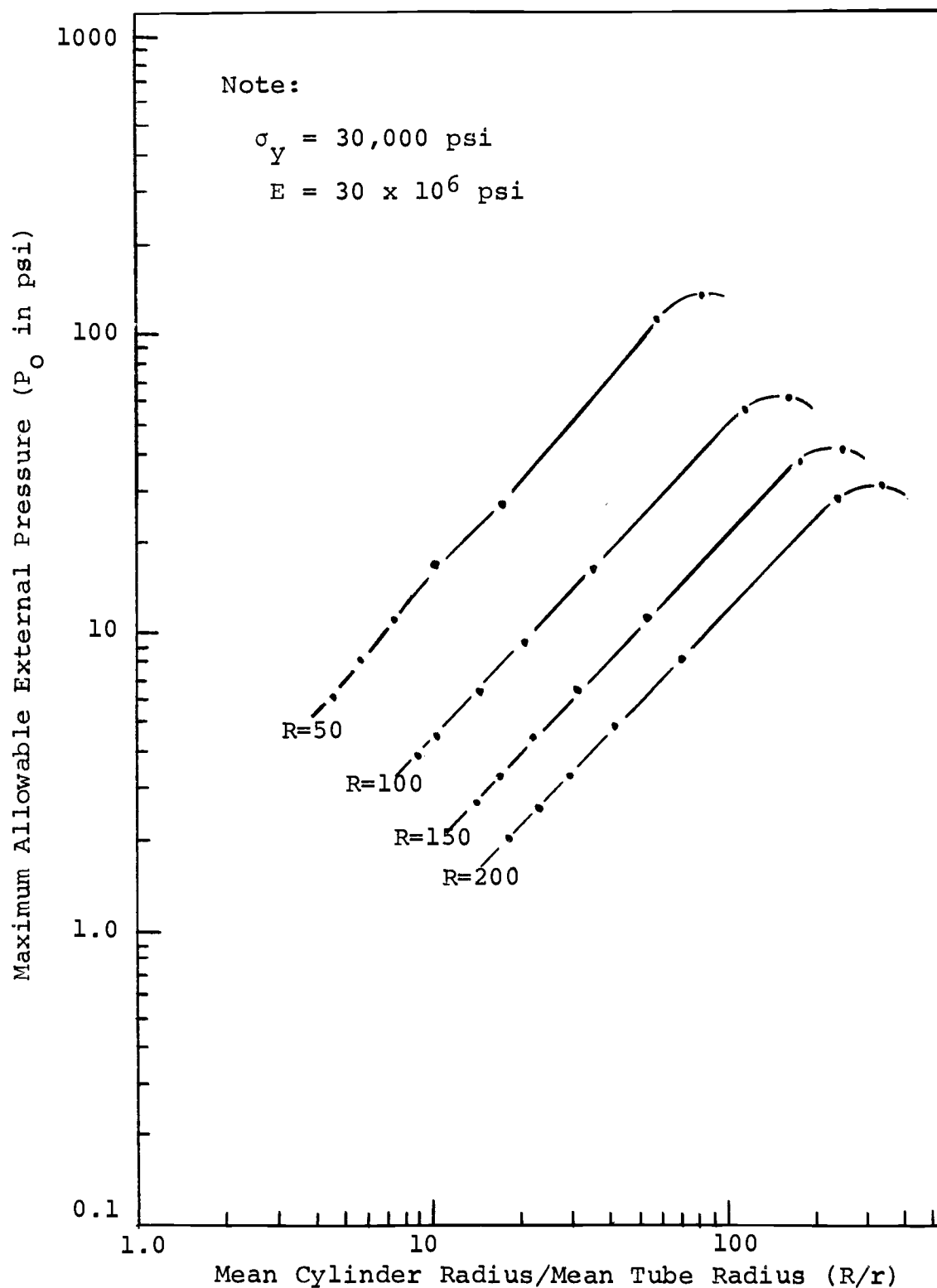


Figure 8. Plot of  $P_o$  vs.  $R/r$  for a prestressed cylinder with a tube wall thickness of 0.30 inches.

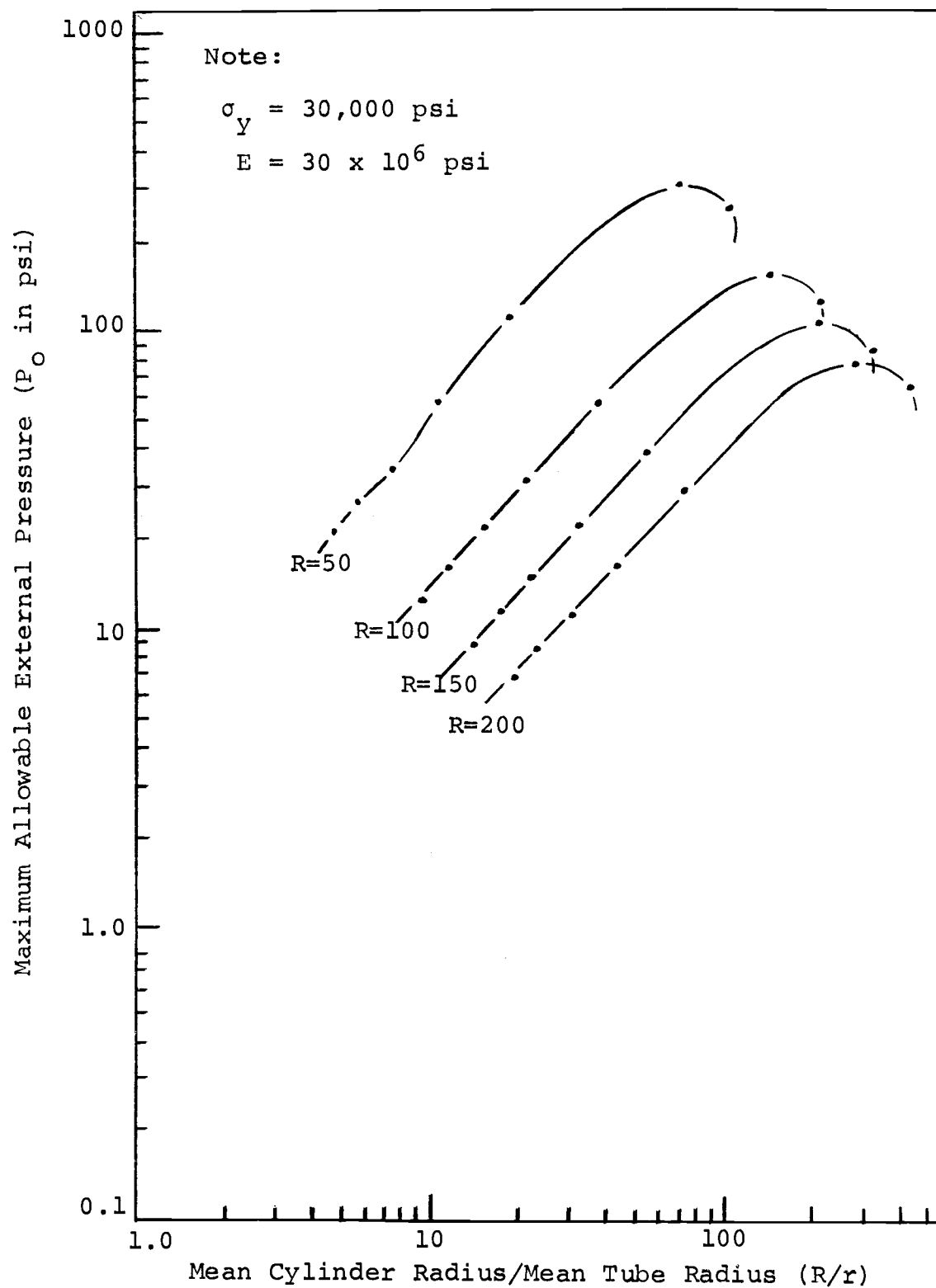


Figure 9. Plot of  $P_o$  vs.  $R/r$  for a prestressed cylinder with a tube wall thickness of 0.55 inches.

prestressing system. This point is seen to vary with both the cylinder radius, and the tube wall thickness. It can also be seen that this characteristic is not present in the plots of Figure 7. The existence of an absolute maximum value of external pressure appears to be directly related to the thickness of the tube wall, since all of the plots in Figures 7, 8, and 9 were made using the same tube radii, and the same cylinder radii.

The discovery that there are what appear to be absolute maximum values of external pressure for some tube and cylinder geometries is a very important one. This means that it may be possible to optimize the design of a prestressed cylinder of a given size. The optimization would come in being able to select both the best tube radius, and the best wall thickness for a given cylinder radius. It would also be possible to determine the best cylinder size if the only criterion for selection was the external pressure that could be withstood. The major difficulty with this optimization procedure is that the solutions are essentially trial and error, but this problem is not major if a high speed computer is available. It should also be noted that there may not be an absolute maximum, as seems to be the case in Figure 7. Maximum values such as those that occur for the plots in Figures 8 and 9 may also exist for the curves in Figure 7, but they are not evident from the points that were calculated. The actual data used to obtain these curves may be found in Appendix III.

#### IV. ANALYSIS OF CONVENTIONAL CYLINDRICAL SHELLS

There are two major areas of concern in the analysis of conventional cylindrical shells, just as there was for prestressed shells. These two regions are the buckling behavior of the cylinder, and the yielding of the cylinder wall. Unlike the prestressed cylinder, the investigation of the modes of failure for a conventional cylindrical shell consists of an analysis of the behavior of the overall cylinder. What is actually meant by a conventional cylindrical shell is shown in Figure 10.

The von Mises Yield Criterion was used for the failure analysis of the cylinder wall, as was done for the prestressed cylinder. Failure was also considered to occur when an element in the cylinder wall begins to yield. For this analysis the cylinder was considered to be thin-walled (i.e., the wall thickness is less than one-tenth of the inside diameter of the cylinder [11]). This was done because in most applications the cylinders being considered are thin-walled. This assumption also will greatly simplify the actual analysis, because a great deal of information is available concerning thin-walled cylinders. The greatest benefit was obtained in the area of buckling. A large amount of work has been done with respect to the buckling of thin-walled cylinders (for example, see references [8] and [14]), and this information is readily available, and

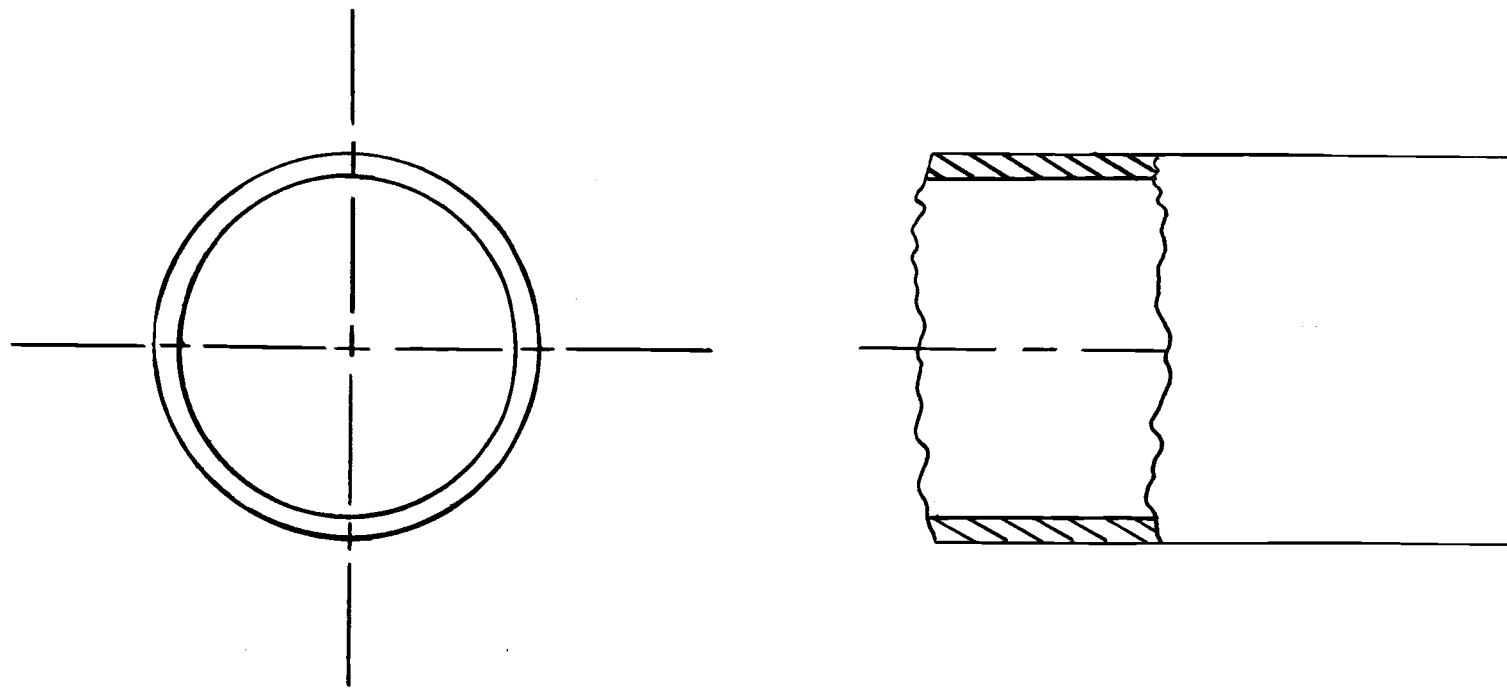


Figure 10. Conventional cylinder.

easily understood. An even greater amount of work has been done on the stress analysis of thin-walled cylinders, and the use of the required equations is a fairly routine matter.

Some further assumptions were made concerning the cylinder itself. For the purposes of analysis, the cylinder was considered to have closed ends, and to only be subjected to hydrostatic (uniform) external pressure. It was also considered to be simply supported, and perfectly rigid. The latter assumption means that there are no displacements or the resulting stresses, due to the cylinder's own weight.

V. RESULTS OF THE ANALYSIS OF A CONVENTIONAL  
CYLINDRICAL SHELL

The analysis of the buckling behavior of a conventional cylindrical shell was based on the work of Flugge [8] and Timoshenko [14]. By going through the same type of analysis that was used for buckling of the tube wall, and keeping only principal terms in the resulting equation, the following expression for  $P_o$  is obtained

$$\begin{aligned} P_o = & \frac{Et}{R} \left[ \frac{1}{n^2 + 0.5 \left( \frac{\pi R}{L} \right)^2} \right] \left\{ \frac{1}{\left[ \left( \frac{nL}{\pi R} \right)^2 + 1 \right]^2} \right. \\ & \left. + \left[ \frac{t^2}{12R^2(1 - \nu^2)} \right] [n^2 + \left( \frac{\pi R}{L} \right)^2]^2 \right\} \end{aligned} \quad (15)$$

where  $P_o$  is the critical external pressure above which buckling will occur, and  $L$  is the length of the cylinder. The quantity  $2n$  is the number of circumferential half-waves into which the cylinder will buckle [where  $n$  is the quantity used in Equation (15)].

Equation (15) is evaluated by determining the value of  $n$  (which must be a positive integer) which minimizes the value for  $P_o$ . The value of  $n$  itself can be determined in one of two ways. The first method is to use the chart shown in Figure II-1 of Appendix II. The second method is to differentiate Equation (15) with respect to  $n$ , and set the resulting equation equal to zero. This results in the following expression

$$\begin{aligned}
 0 = & \left(\frac{6}{F^6}\right)n^{11} + \left(\frac{28}{F^4}\right)n^9 + \left(\frac{52}{F^2}\right)n^7 + 48n^5 \\
 & + (22F^2 - \frac{6G}{F^2})n^3 + (4F^4 - 4G)n
 \end{aligned} \tag{16}$$

where

$$F = \frac{\pi R}{L}$$

$$G = \frac{12R^2(1 - v^2)}{t^2}$$

and all other terms are as previously defined. The value of n to use in Equation (15) is determined from Equation (16) by an iteration process. Since n is constrained to be an integer the equality of Equation (16) will in general not hold true. If this is the case, the value of n which should be used is the value which results in a change in sign of the remainder calculated using Equation (16) (i.e., if the value which satisfies the equality of Equation (16) is between n<sub>1</sub> and n<sub>2</sub>, with n<sub>2</sub> being greater than n<sub>1</sub>, the value that should be used for n is n<sub>2</sub>, remembering that n must be an integer).

The failure analysis of a conventional cylindrical shell consists of an investigation of the stresses present in the shell wall. Based on the assumption that the cylinder is thin-walled, with closed ends, the following stresses are obtained

$$\sigma_r = 0$$

$$\sigma_{\theta} = - \frac{P_o R}{t}$$

$$\sigma_x = - \frac{P_o R}{2t}$$

Solving for the external pressure using the von Mises Yield Criterion, and assuming that yielding and failure are synonymous results in the following equation

$$P_o = \frac{2t \sigma_y}{\sqrt{3} R} \quad (17)$$

where  $P_o$  is the external pressure above which yielding will occur.

The maximum allowable value of external pressure for the conventional cylinder is determined in much the same manner as it was for the prestressed cylinder. That is, the two values of  $P_o$  are calculated using Equations (15) and (17). These values are then compared, with the smallest of the two being used as the value for the maximum external pressure.

## VI. COMPARISON OF RESULTS

Before any comparisons can be made between a conventional cylinder and one that is prestressed, a common basis for the comparison must be decided upon. It was decided that the best way to compare the two different types of cylinder (prestressed and conventional) was on the basis of total mass. This was chosen, because it was felt that it would give the most valid comparison, and yield the most valuable information. In effect, what will be done is to make a comparison between two different types of cylinders (i.e., conventional and prestressed) both having the same mean radius, same length, and equal masses.

The mass of an object is equal to the volume of material the object is made up of, multiplied by the density of the material. From the above definition, the first step in the comparison will be to determine the volume of material that the prestressed cylinder contains.

$$N = \text{Number of Coils} = \frac{L}{2r_o}$$

$$A = \text{Cross-sectional Area of the Tubing} = 2\pi r_i t$$

$$C = \text{Length of a Single Coil} = 2\pi R$$

$$V = \text{Total Volume of Material} = NCA = \frac{2\pi^2 L R t r_i}{r_o}$$

All other terms used in the above equations are the same as those previously defined.

If we assume that the two cylinders being compared are constructed from the same material, then the volume of material in each is all that need be compared. For a conventional cylinder

$$V = 2\pi RLt'$$

where  $t'$  is the wall thickness of the conventional cylinder. Equating the two volumes and solving for  $t'$  results in

$$t' = \frac{\pi r_i t}{r_o} = \frac{\pi t}{\rho} \quad (18)$$

where  $\rho$  is as previously defined. Equation (18) is an expression for the equivalent wall thickness that a conventional cylinder must possess in order to have the same mass as a prestressed cylinder of the same major dimensions (i.e., length and mean radius).

Comparisons can now be made based on the total mass of the cylinders, by making use of Equation (18), and the assumption that allowed its derivation. The same values that were used to obtain the plots shown in Figures 7 through 9 will again be used to make comparisons. Figures 11 through 13 show the results of the comparisons based on the assumption of equal total masses for both cylinders. Again, it should be noted that both the horizontal and vertical scales are logarithmic, and that the length of the cylinder was assumed to be equal to its radius.

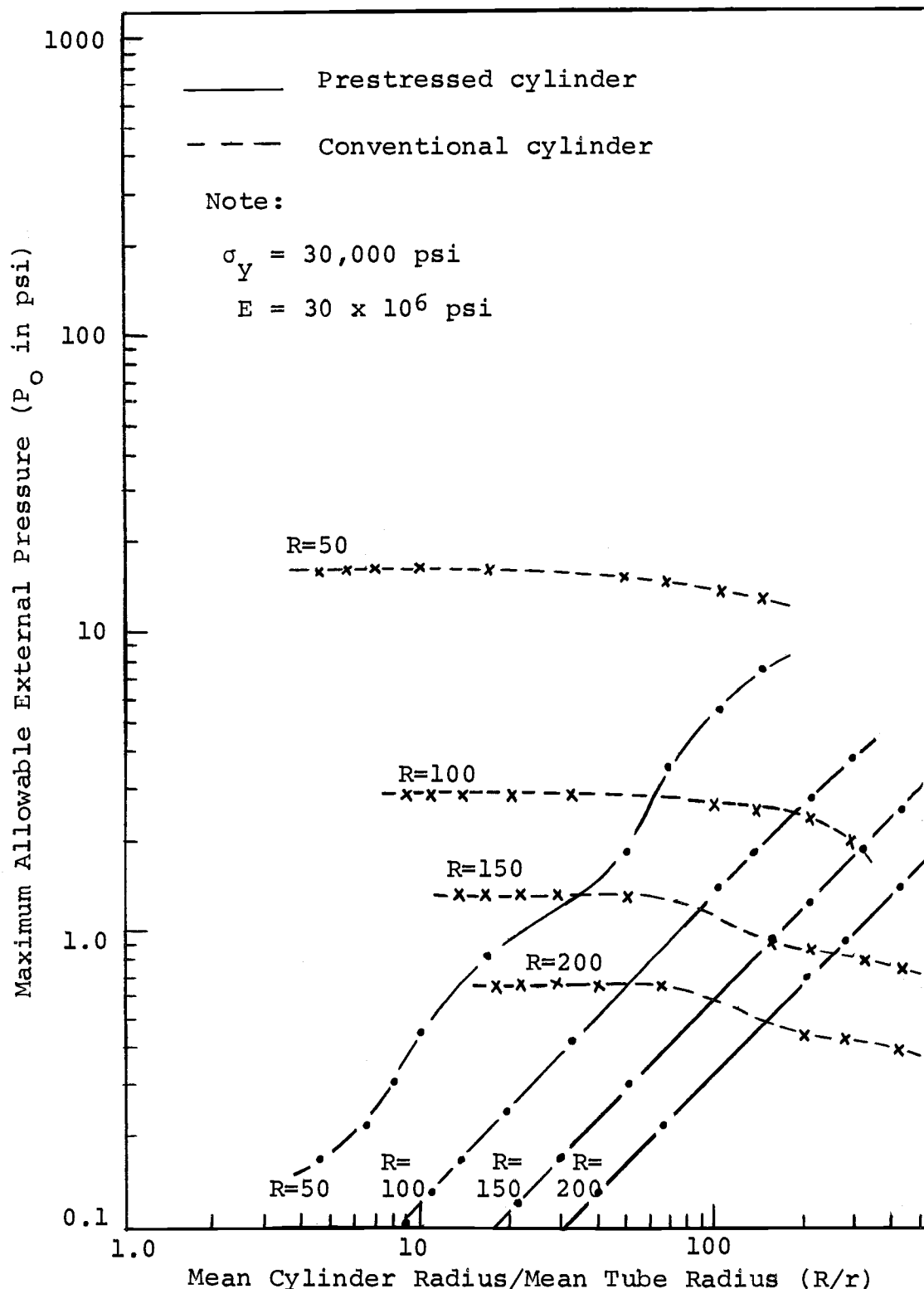


Figure 11. Plot of  $P_o$  vs.  $R/r$  for conventional and prestressed cylinders with a tube wall thickness of 0.05 inches.

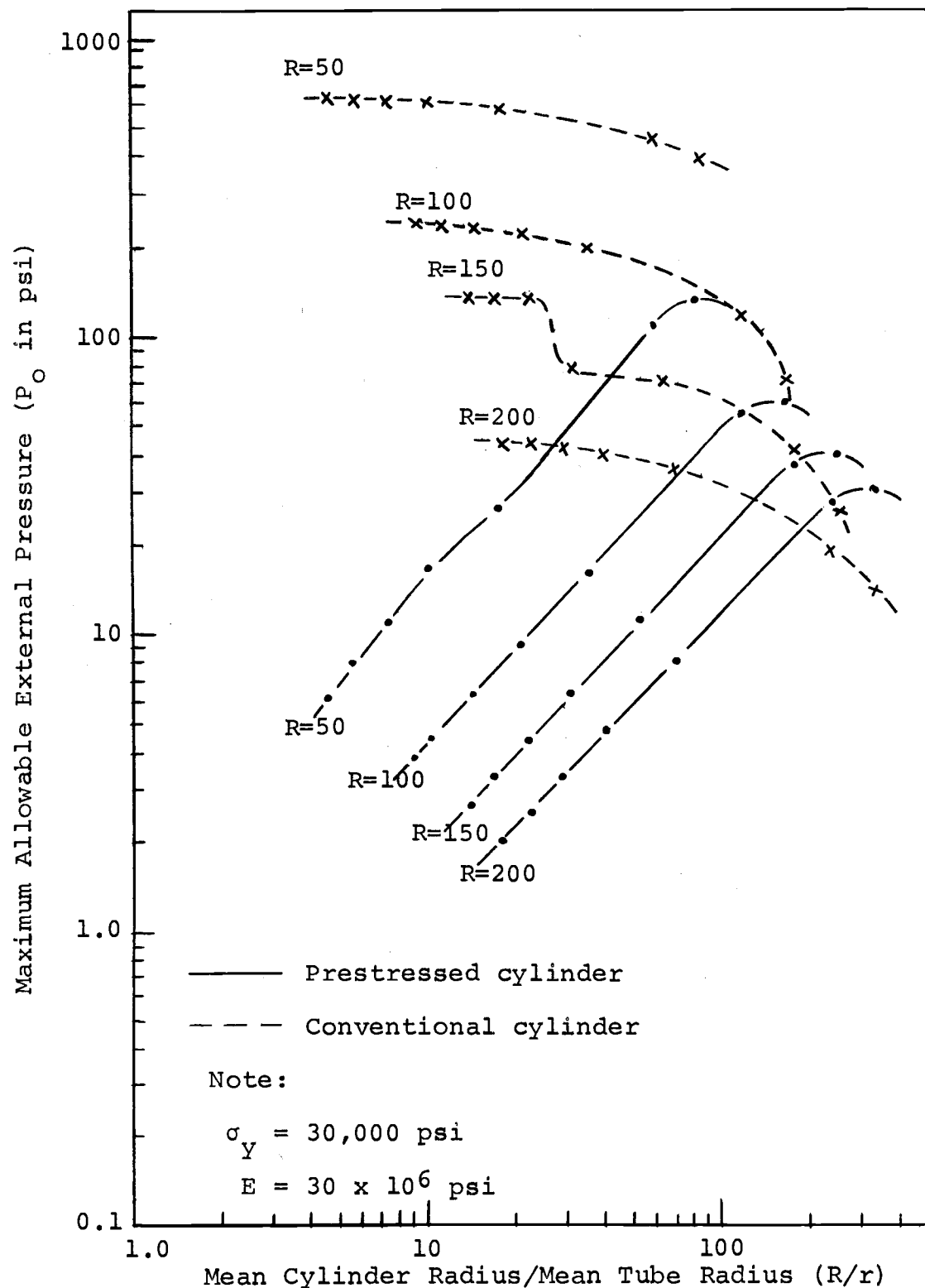


Figure 12. Plot of  $P_o$  vs.  $R/r$  for conventional and prestressed cylinders with a tube wall thickness of 0.30 inches.

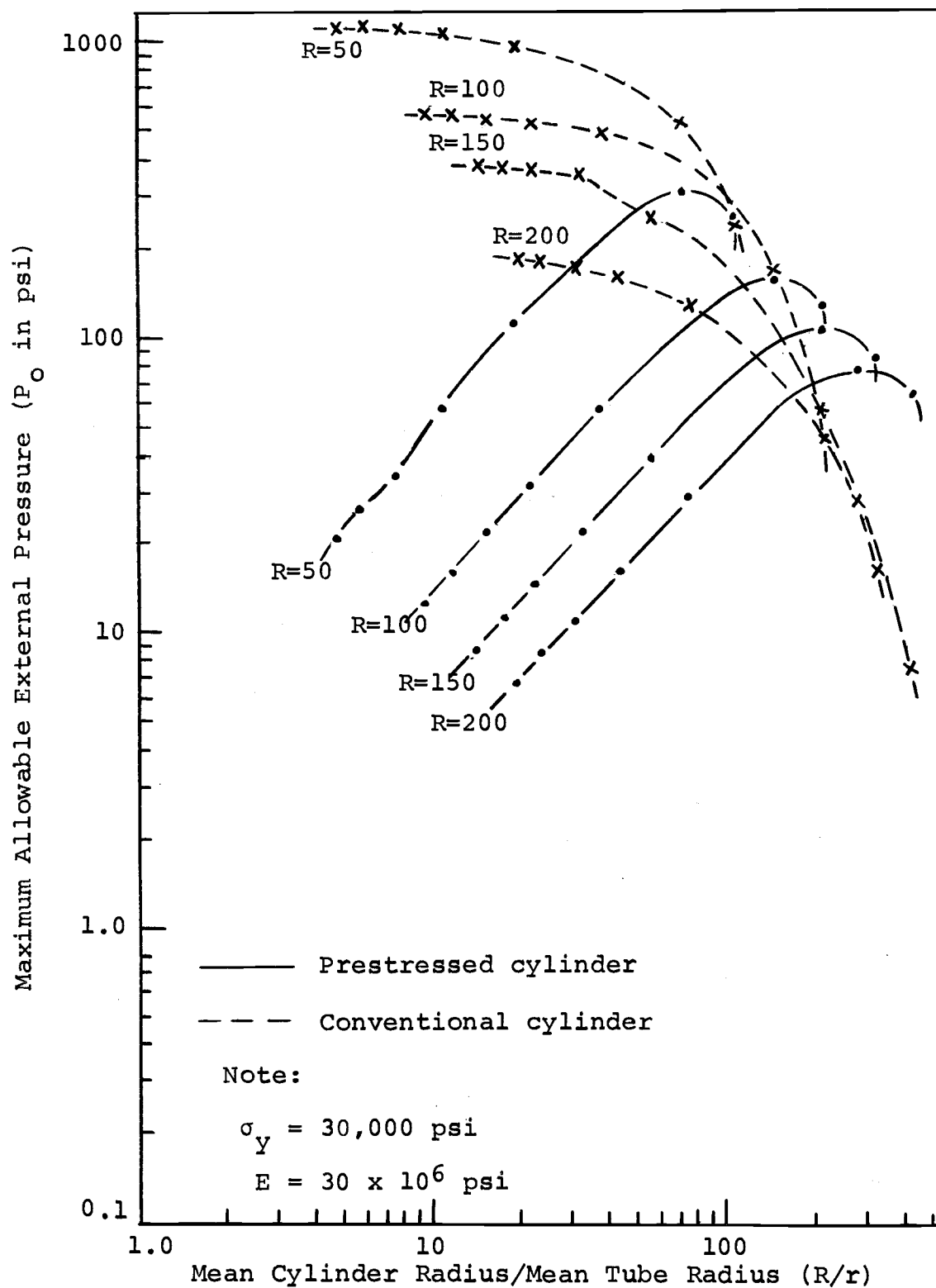


Figure 13. Plot of  $P_o$  vs.  $R/r$  for conventional and prestressed cylinders with a tube wall thickness of 0.55 inches.

There are several things that are immediately obvious when viewing the plots shown in Figures 11 through 13. The first of these is the large jump that occurs in the allowable external pressure ( $P_o$ ) for a conventional cylinder of mean radius 150 inches in Figures 12 and 13. These large steps are due to a change in failure modes. To the right of the step (in the direction of increasing  $R/r$ ) the buckling behavior of the cylinder determines the maximum  $P_o$ , but to the left of the step the maximum  $P_o$  is determined by yielding of the wall material. Another readily observable fact is that the allowable external pressure increases as the tube thickness increases (which also means the wall thickness of the conventional cylinder increases). It is also evident that the maximum external pressure for a conventional cylinder drops off quite rapidly past a certain point. This effect can be readily seen in Figure 13, and is in evidence in Figure 12 to a lesser extent. This behavior is hinted at in Figure 11, but it cannot be said with assurance that it will occur. This rapid drop-off is due to the thinning of the cylinder wall which is a result of the decreasing tube radius (see Equation (18) for the relationship between the wall thickness of a conventional cylinder, and the tube radius of a prestressed cylinder).

The most important results are obtained when the curves for a conventional cylinder, and those for a prestressed cylinder of the same length, mean radius, and mass

are compared. First, Figure 11 will be examined. It can be seen that the two sets of curves intersect one another for cylinder radii of 100, 150, and 200 inches, with the conventional cylinder being superior (from the viewpoint of allowable external pressure) below a certain value of  $R/r$  and the prestressed cylinder superior above that point. The preceding observations do not apply to the set of curves for a radius of 50 inches, because these two curves do not intersect at any point (they may intersect at larger values of  $R/r$  though).

Basically the same things that were evident in Figure 11 are also evident in Figure 12. This being that the curves for a conventional cylinder of radii 150 and 200 inches intersect with the ones for a prestressed cylinder of equivalent radii. It also appears that the two curves for a radius of 100 inches will intersect one another, but care must be taken when interpolating past the last calculated point. It can also be seen from the plots in Figure 12 that the maximum allowable value of  $P_o$  for a conventional cylinder drops off much more rapidly than in Figure 11. Also, the curves for a prestressed cylinder appear to have absolute maximum values, as was discussed in Section IV.

The curves of Figure 13 also seem to follow the same general pattern that was evident in Figures 11 and 12. This pattern being that the curves for prestressed and

conventional cylinders of 150 and 200 inch radii intersect one another. It can also be seen that the respective curves for radii of 50 and 100 inches have points of intersection. The pattern of the maximum  $P_o$  for a conventional cylinder dropping off with increasing values of  $R/r$  is also evident, but much more pronounced than in Figures 11 and 12. The appearance of absolute maximum values for the prestressed cylinder curves can also be seen in Figure 13, just as they were in Figure 12.

There are several important conclusions that can be drawn from the preceding comparisons. The first, and a very important one, is that a prestressed cylinder is superior to a conventional cylinder in some instances, as far as the maximum allowable value of external pressure is concerned. Examples of this can be seen in each of Figures 11, 12 and 13, where portions of the curve for a prestressed cylinder lie above an equivalent portion for a conventional cylinder of equal radius.

The second important conclusion involves the tube radius, tube wall thickness, and cylinder radius. It appears that the prestressing system has an advantage over a conventional cylinder when the tube wall is thin, and the radius of the tube is small when compared with the cylinder radius. The apparent reason for this is that at small values of tube wall thickness and tube radius, the equivalent wall thickness of the conventional cylinder is also

quite small. It is also apparent from examination of Figures 11 through 13, that the best results obtained in using the prestressing system, as compared to using a conventional cylinder, is when the cylinder radius is large.

A third, and most important conclusion can be drawn concerning the overall comparison of a prestressed cylinder and conventional cylinder. It appears from the data plotted in Figures 11 through 13 that a cylinder using a tubular prestressing system is superior to a conventional cylinder if the tube wall is relatively thin, the tube radius is fairly small, and the mean cylinder radius is large. What this really means is, that a prestressed cylinder may very well be superior to a conventional cylinder, from the standpoint of the maximum allowable external pressure, if the overall mass of the cylinder is of prime concern. This appears to be true, because the mass of a cylinder of a given radius and length will decrease as the radius and wall thickness of the tubing it is constructed from decreases.

## VII. CONCLUSIONS

There are two important conclusions that can be reached concerning a prestressed cylindrical shell. The first, and most obvious is that prestressing a cylinder subject to external pressure, by constructing it from coiled pressurized tubing, appears to be a valid and workable solution. This has been shown to be true, based on a theoretical analysis of the pressure induced forces acting on the cylinder itself. This analysis included both buckling and yielding considerations for the tubing that makes up the cylinder.

The second conclusion is that a prestressed cylindrical shell is superior in some instances to a conventional cylindrical shell of equal diameter, length and mass. This was shown to be true through comparisons between prestressed cylinders and conventional cylinders of equal size and mass, for arbitrary cylinder and tube geometries. It was further shown that a prestressed cylinder appears to be better than a conventional cylinder if the cylinder under consideration has a large diameter, and its mass is of prime importance.

There is much work that must be done before the concept of prestressing a cylinder by constructing it from coiled pressurized tubing is in truth a feasible and realistic idea. Much of this work needs to be in the area of improving the models used for analysis. Things such as shape imperfections in the tubing, and irregularities in the

cylinder itself must be taken into account. Other areas that must also be looked into are pressure irregularities on the cylinder surface, and the effects of the cylinder weight (which was neglected for this investigation). Other applications for this type of prestressing system, such as using it to stiffen a conventional cylinder, or covering the tubular structure with a smooth hull should also be looked in to. All in all, this investigation was only a preliminary one, and much more work still remains to be done.

## BIBLIOGRAPHY

1. Batdorf, S. B. A Simplified Method of Elastic-Stability Analysis for Thin Cylindrical Shells. National Advisory Committee for Aeronautics, Report 874, 1947, p. 285-309.
2. Baumeister, Theodore (ed.). Standard Handbook for Mechanical Engineers. 7th ed. New York, McGraw-Hill, 1967. 2456 p.
3. Beckwith, T. G., N. Lewis Buck. Mechanical Measurements. Reading, Mass., Addison-Wesley, 1969. 642 p.
4. Bergman, E. O., et al. (eds.). Pressure Vessels and Piping Design-Collected Papers 1927-1959. New York, American Society of Mechanical Engineers, 1960. 710 p.
5. Bohm, G. J., et al. (eds.). Pressure Vessels and Piping: Design and Analysis. Vol. I, Analysis. New York, American Society of Mechanical Engineers, 1972. 754 p.
6. Crandall, Stephen H., Norman C. Dahl, Thomas J. Lardner (eds.). An Introduction to the Mechanics of Solids. 2d ed. New York, McGraw-Hill, 1972. 628 p.
7. Dahlke, Otto P. H. Concept of a Prestressed Tubular Hull Structure. Martin Company, Denver, Colorado, March 1964.
8. Flugge, Wilhelm. Stresses in Shells. 2d ed. Berlin, Springer Verlag, 1962. 499 p.
9. Gill, S. S. (ed.). The Stress Analysis of Pressure Vessels and Pressure Vessel Components. New York, Pergamon Press, 1970. 592 p.
10. Mendelson, Alexander. Plasticity: Theory and Application. New York, MacMillan, 1968. 353 p.
11. Roark, Raymond J. Formulas for Stress and Strain. 4th ed. New York, McGraw-Hill, 1965. 432 p.
12. Selby, Samuel M. Standard Mathematical Tables. 12th ed. Cleveland, Ohio, Chemical Rubber Co., 1972. 705 p.

13. Steele, C. R. Toroidal Pressure Vessels. *Journal of Spacecraft and Rockets.* 2:937-943, 1965.
14. Timoshenko, Stephen P., James M. Gere. Theory of Elastic Stability. 2d ed. New York, McGraw-Hill, 1961, 541 p.
15. Timoshenko, Stephen P., J. N. Goodier. Theory of Elasticity. 2d ed. New York, McGraw-Hill, 1970. 567 p.
16. Timoshenko, Stephen P., S. Woinowsky-Krieger. Theory of Plates and Shells. 2d ed. New York, McGraw-Hill, 1959. 580 p.
17. Transactions of the American Society of Mechanical Engineers, ser. E. *Journal of Applied Mechanics,* 1960-1973.
18. Widenburg, Dwight F., Charles Trilling. Collapse by Instability of Thin Cylindrical Shells Under External Pressure. *Transactions of the American Society of Mechanical Engineers.* 56:819-826, 1934.
19. Wylie, C. R. Advanced Engineering Mathematics. 3d ed. New York, McGraw-Hill, 1966. 813 p.

## **APPENDICES**

APPENDIX I  
PRESTRESSED CYLINDRICAL SHELL ANALYSIS  
A. Buckling

See Figure I-1 for the model on which the following analysis is based. Figure I-2 shows the element on which the analysis of buckling is based. From summation of forces (assuming the cylinder is stationary) for the element shown in Figure I-2

$$\begin{aligned}
 \Sigma F_r = & N_\theta \Delta x \sin \alpha|_{\theta+\Delta\theta} - N_\theta \Delta x \sin \alpha|_\theta + V_\theta \Delta x \Delta r \cos \alpha|_{\theta+\Delta\theta} \\
 & - V_\theta \Delta x \Delta r \cos \alpha|_\theta + P_r r \Delta \theta \Delta x|_{r+\Delta r} - P_r r \Delta \theta \Delta x|_r \\
 & + N_x r \Delta \theta \sin \beta|_{x+\Delta x} - N_x r \Delta \theta \sin \beta|_x - V_x r \Delta \theta \Delta r \cos \beta|_{x+\Delta x} \\
 & + V_x r \Delta \theta \Delta r \cos \beta|_x = 0
 \end{aligned} \tag{1}$$

Dividing by  $r \Delta x \Delta \theta \Delta r$ , using the small angle assumption ( $\sin \theta = \tan \theta = \theta$ , and  $\cos \theta = 1$ ), and taking limits as  $\Delta x \Delta \theta$  go to zero. Also noting the fact that

$$\alpha = \Delta \theta$$

and the radial component of the circumferential force becomes

$$N_\theta \sin \Delta \theta = N_\theta \Delta \theta$$

due to the uniform compression of the element. If we also let  $r$  go to  $r_i$  and

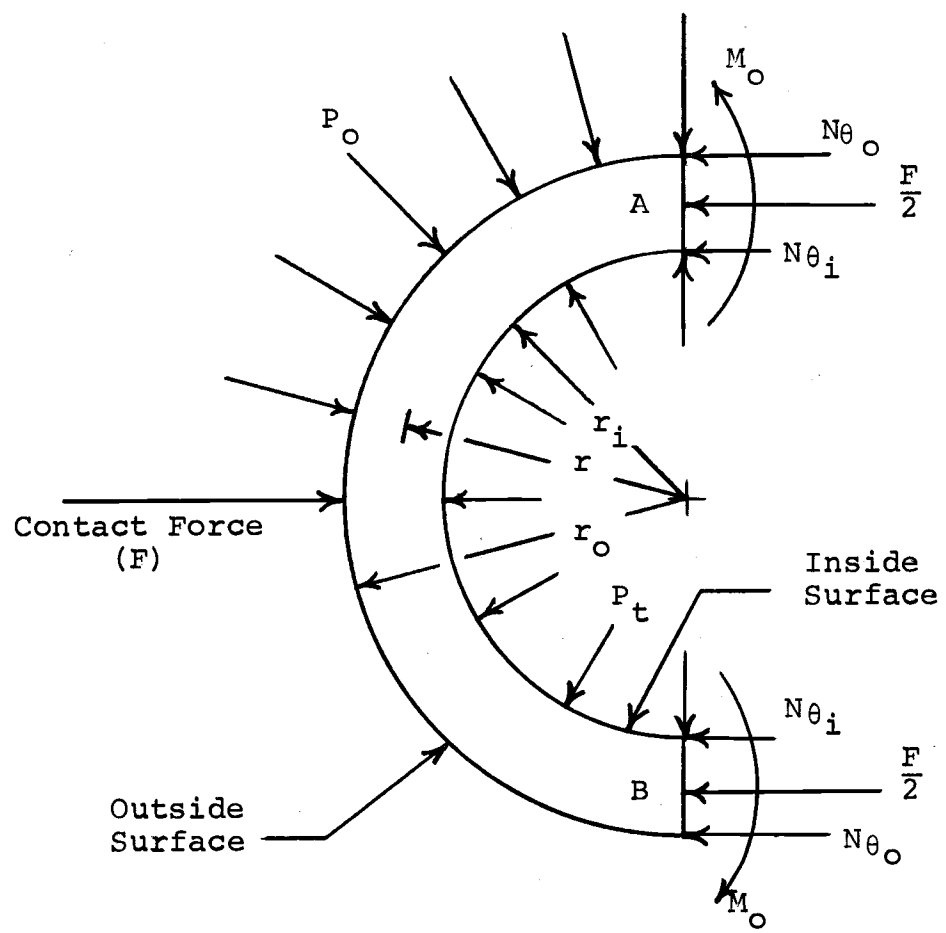


Figure I-1. Model of loaded tubing.

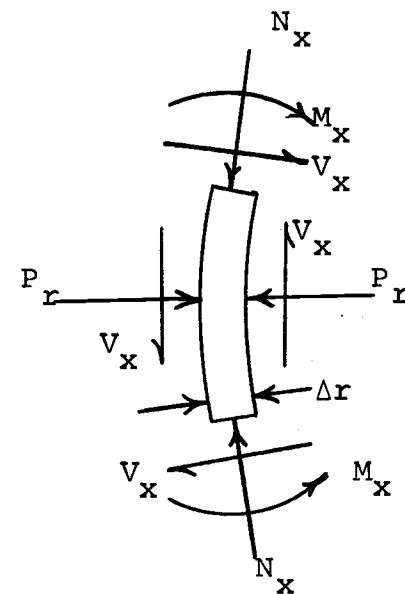
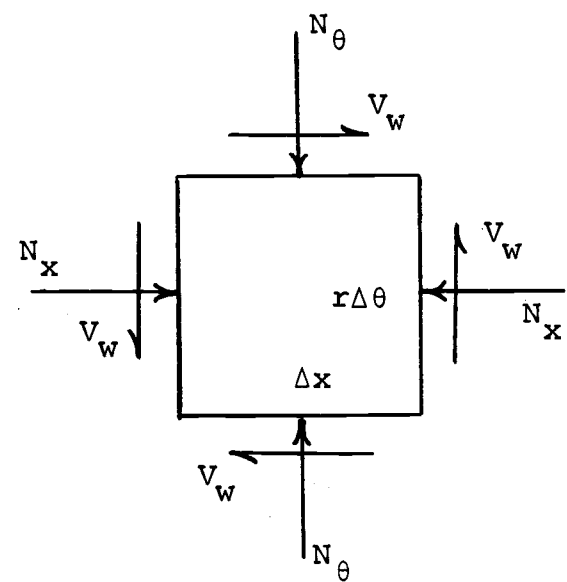
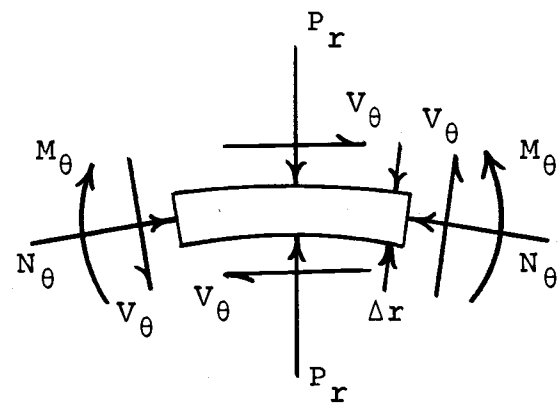


Figure I-2. Tube wall element.

$$\tan \beta = \frac{\partial W}{\partial X}$$

where W is the radial deflection. The resulting equation is

$$\frac{1}{r_i \Delta r} \frac{\partial (N_\theta \Delta \theta)}{\partial \theta} + \frac{1}{r_i} \frac{\partial V_\theta}{\partial \theta} + \frac{\partial P_r}{\partial r} + \frac{1}{\Delta r} \frac{\partial (N_x \frac{\partial W}{\partial X})}{\partial X} - \frac{\partial V_x}{\partial X} = 0 \quad (2)$$

Using the relations

$$V_\theta = \frac{1}{r_i} \frac{\partial M_\theta}{\partial \theta} \quad \text{and} \quad V_x = \frac{\partial M_x}{\partial X}$$

and assuming  $N_\theta$ ,  $N_x$  are constant, Equation (2) becomes

$$\frac{N_\theta}{r_i \Delta r} + \frac{1}{r_i^2} \frac{\partial^2 M}{\partial \theta^2} + \frac{\partial P_r}{\partial r} + \frac{N_x}{\Delta r} \frac{\partial^2 W}{\partial X^2} - \frac{\partial^2 M_x}{\partial X^2} = 0 \quad (3)$$

If we assume that the shell is uniformly compressed, the change in curvature in the circumferential direction is very small (essentially zero). If this is true, the moments in the circumferential direction are constant. Therefore

$$V_\theta = \frac{1}{r_i} \frac{\partial M_\theta}{\partial \theta} = 0$$

Using this fact, and the fact that  $\Delta r$  is equal to the thickness of the tube wall (t) in the limiting case, Equation (3) becomes

$$\frac{N_\theta}{r_i t} + \frac{\partial P_r}{\partial r} + \frac{N_x}{t} \frac{\partial^2 W}{\partial X^2} - \frac{\partial^2 M_x}{\partial X^2} = 0 \quad (4)$$

Also,

$$M_x = - \frac{D \partial^2 W}{\partial x^2}$$

where

$$D = \frac{Et^3}{12(1-\nu^2)}$$

Therefore, Equation (4) becomes

$$D \frac{\partial^4 W}{\partial x^4} + \frac{N_x}{t} \frac{\partial^2 W}{\partial x^2} + \frac{N_\theta}{r_i t} = - \frac{\partial P_r}{\partial r} \quad (5)$$

The quantity  $\partial P_r / \partial r$  can be approximated by

$$\frac{\partial P_r}{\partial r} = \frac{\Delta P_r}{\Delta r} = \frac{P_t - P_o}{t}$$

The equation in final form is

$$Dt \frac{\partial^4 W}{\partial x^4} + N_x \frac{\partial^2 W}{\partial x^2} + \frac{N_\theta}{r_i} = P_o - P_t \quad (6)$$

By using Hooke's Law, and the fact that

$$N_x = \sigma_x t$$

$$N_\theta = \sigma_\theta t$$

it can be shown that

$$N_\theta = \frac{WtE}{r_i} + \nu(N_x + t\sigma_r)$$

where

$$\sigma_r = \text{radial stress}$$

Substituting this into Equation (6), and solving for W (the radial displacement)

$$\begin{aligned} W_1(x, \theta) = & C_1 \cos \sqrt{A_1}x + C_2 \sin \sqrt{A_1}x + \cos \sqrt{A_2}x \\ & + C_4 \sin \sqrt{A_2}x + \frac{Cr_i^2}{Et} \end{aligned} \quad (7)$$

where

$$A_1 = -\frac{Nx}{2Dt} + \sqrt{\frac{Nx^2}{4D^2t^2} - \frac{E}{Dr_i^2}}$$

$$A_2 = -\frac{Nx}{2Dt} - \sqrt{\frac{Nx^2}{4D^2t^2} - \frac{E}{Dr_i^2}}$$

$$C = \frac{(P_o - P_t)}{t} - \frac{v}{r_i} (N_x + t\sigma_r)$$

and D is as previously defined.

The equation for the radial deflection [Equation (7)] only takes into account the forces, moments, and deflections caused by the external and tube pressures acting directly on the tube wall. For a complete analysis, the contact forces between the coils of tubing must also be taken into account. The model used for the analysis based on these contact forces may be found in Figure I-3. Using this model, and the following boundary conditions

$$1. \quad \frac{\partial W_2}{\partial \theta} \Big|_{\theta=0} = 0$$

$$2. \quad \frac{\partial W_2}{\partial \theta} \Big|_{\theta=\frac{\pi}{2}} = 0$$

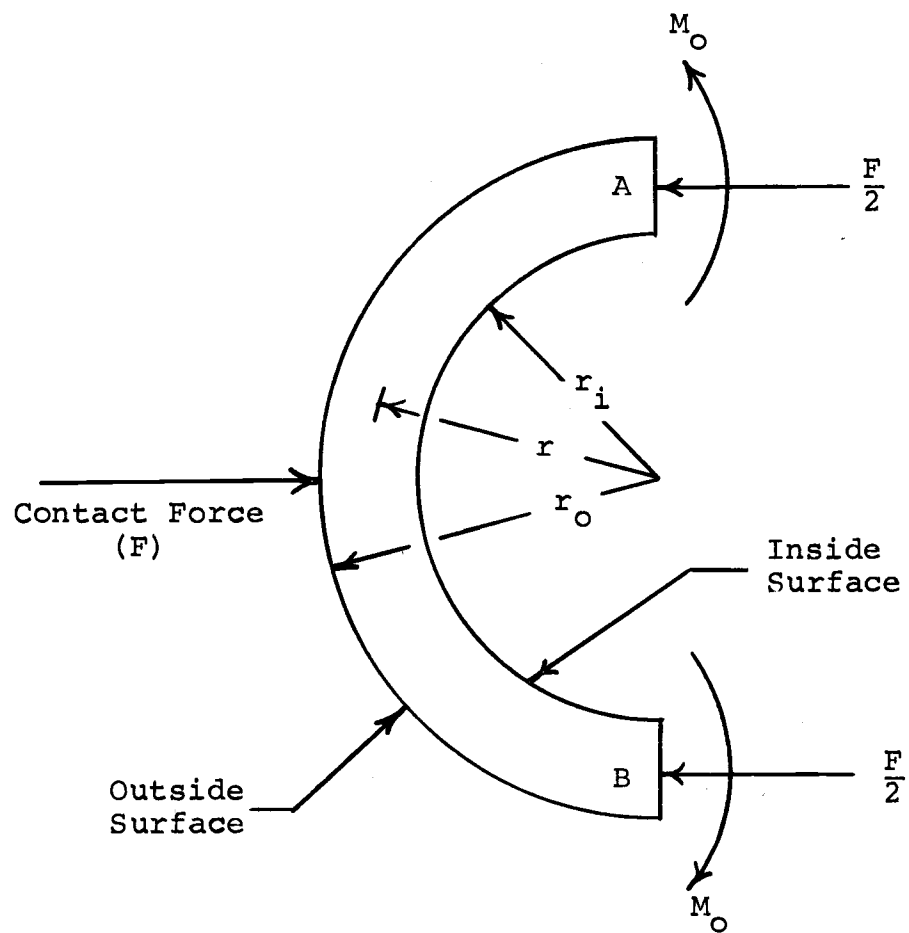


Figure I-3. Model showing only contact forces and resulting moments.

it can be shown that

$$w_2(x, \theta) = \frac{3\pi}{2} \frac{Fr^3(1 - v^2)}{Et^3} \cos \theta + \frac{3Fr^3(1 - v^2)}{Et^3} (\sin \theta \\ - \theta \cos \theta) - \frac{6(1 - v^2)r^2}{Et^3} (2M_o + Fr)$$

Using the principles of superposition

$$w(x, \theta) = w_1(x, \theta) + w_2(x, \theta)$$

Solving the equation for the radial displacement using the following boundary conditions

$$1. \quad w(0, \theta) = 0$$

$$2. \quad \frac{\partial w(0, \theta)}{\partial x} = f(P_o, P_t) \text{ where } f(P_o, P_t) \text{ is bounded as } x \text{ goes to infinity.}$$

$$3. \quad \frac{\partial^2 w(0, \theta)}{\partial x^2} = \text{Moment} = 0$$

$$4. \quad \frac{\partial^3 w(0, \theta)}{\partial x^3} = \text{Shear} = 0$$

results in the following equation

$$w(x, \theta) = \frac{KA_2}{A_1 - A_2} (\cos \sqrt{A_1}x - \frac{A_1}{A_2} \cos \sqrt{A_2}x) \\ - \frac{A_2 f(P_o, P_t)}{\sqrt{A_1}(A_1 - A_2)} (-\sin \sqrt{A_1}x + [\frac{A_1}{A_2}]^{3/2} \sin \sqrt{A_2}x) \\ + [(\frac{P_o - P_t}{t} - \frac{v}{r_i} (N_x + t\sigma_r))] \frac{r_i^2}{Et} \\ + \frac{3\pi}{2} \frac{Fr^3(1 - v^2)}{Et^3} \cos \theta \quad (8)$$

$$+ \frac{3Fr^3(1 - v^2)}{Et^3} (\sin \theta - \theta \cos \theta)$$

$$- \frac{6(1 - v^2)r^2}{Et^3} (2M_o + Fr)$$

where  $K$  is a function of all terms, not a function of  $x$ .

Buckling is said to occur when the deflections of the shell tend to grow indefinitely [14]. Since all the terms in Equation (8) are finite, the only possible solution for buckling to occur is when

$$A_1 = A_2$$

Solving this equation, it can readily be found that

$$N_x = \pm \frac{Et^2}{r_i} \sqrt{\frac{t}{3(1 - v^2)}} \quad (9)$$

It can also be shown that

$$N_x = \frac{P_{tri}}{2} - \frac{P_o(R + r_o)r_o}{\pi r_i} = \frac{P_{tri}}{2} - \frac{P_o R_o \rho}{\pi} \quad (10)$$

Combining equations (9) and (10) results in

$$P_o = \frac{\pi}{R_o \rho} \left[ \frac{P_{tri}}{2} + Et(\rho - 1) \sqrt{\frac{t}{3(1 - v^2)}} \right] \quad (11)$$

This equation indicates that the maximum external pressure allowed from buckling considerations increases linearly as a function of the tube pressure for a given cylinder geometry.

### B. Yielding

It is also possible that failure (yielding) of the tubing material occurs prior to buckling. The von Mises Yield Criterion (Distortion Energy) will be used throughout the analysis.

#### Inner Surface

$$\sigma_r = -P_t$$

$$\sigma_\theta = \sigma_{\theta 1} - \sigma_{\theta 2}$$

$$\sigma_{\theta 1} = \frac{P_t(\rho^2 + 1) - 2P_o\rho^2}{\rho^2 - 1}$$

$$\sigma_{\theta 2} = \frac{F}{2A} - \frac{M_O C}{I}$$

$$\sigma_x = \frac{P_t r_i}{2t} - \frac{P_o \rho R_o}{\pi t} = \frac{P_t}{2(\rho - 1)} - \frac{P_o \rho R_o}{\pi t}$$

The above values are for the portion of the tubing on the outside surface of the cylinder (the surface subjected to the external pressure).

For the portion of the tubing on the inside surface of the cylinder

$$\sigma_r = -P_t$$

$$\sigma_\theta = \sigma_{\theta 1} - \sigma_{\theta 2}$$

$$\sigma_{\theta 1} = \frac{P_t(\rho^2 + 1)}{\rho^2 - 1}$$

$$\sigma_{\theta_2} = \frac{F}{2A} - \frac{M_O c}{I}$$

$$\sigma_x = \frac{P_t}{2(\rho - 1)} - \frac{P_O \rho R_O}{\pi t}$$

where

$$c = \frac{t}{2}$$

$$I = \frac{t^3}{12}$$

$$A = t$$

Using Castigliano's Theorems

$$U = \int_L \frac{M_\theta^2}{2EI} dx$$

and

$$\frac{\partial U}{\partial M_O} = \varphi$$

where  $\varphi$  is the angle of rotation about the axis of the moment vector.

If we assume that the cross section at  $\underline{\theta} = \pi/2$  does not rotate,  $\underline{\varphi}$  is equal to zero, and

$$\frac{\partial U}{\partial M_O} = 0$$

Therefore

$$\frac{1}{EI} \int_0^{2\pi} M_\theta \frac{\partial M_\theta}{\partial M_O} r d\theta = 0. \quad (12)$$

It can easily be shown that

$$M_\theta = M_O + \frac{Fr}{2} (1 - \sin \theta) \quad \text{for } 0 \leq \theta \leq \pi/2$$

Substituting and integrating results in the expression

$$M_O = \frac{Fr}{2} \left( \frac{2}{\pi} - 1 \right) \quad (13)$$

Therefore

$$\sigma_{\theta 2} = \frac{F}{2t} - \frac{3Fr}{t^2} \left( \frac{2}{\pi} - 1 \right)$$

where F is positive for a compressive force as shown in Figure I-1. F can also be expressed as a function of P<sub>O</sub> if we say

$$F = f(P_O) = \varphi P_O$$

where  $\varphi$  is a constant that relates F and P<sub>O</sub>. The quantity  $\varphi$  is positive for a compressive force. Therefore

$$\sigma_{\theta 2} = \frac{\varphi P_O}{2t} - \frac{3\varphi P_O r}{t^2} \left( \frac{2}{\pi} - 1 \right) \quad (14)$$

Substituting these expressions into the von Mises Yield Criterion, we obtain two expressions for the maximum allowable P<sub>O</sub>

$$P_O = - \frac{B_i P_t}{2A_i} \pm \sqrt{\frac{B_i^2 P_t^2}{4A_i^2} + \frac{\sigma_y^2}{A_i} - \frac{C_i P_t^2}{A_i}} \quad (15)$$

where

$$A_i = \frac{\rho R_O}{\pi t} \left[ \frac{\rho R_O}{\pi t} - \frac{2\rho^2}{\rho^2 - 1} - \frac{\varphi}{2t} + \frac{3\varphi r}{t^2} \left( \frac{2}{\pi} - 1 \right) \right] \\ + \left[ \frac{2\rho^2}{\rho^2 - 1} + \frac{\varphi}{2t} - \frac{3\varphi r}{t^2} \left( \frac{2}{\pi} - 1 \right) \right]^2$$

$$\begin{aligned}
 B_i &= \frac{\rho R_o}{\pi t} \left[ \frac{1}{\rho - 1} + \frac{\rho^2 + 1}{\rho^2 - 1} - 1 \right] \\
 &\quad + \left[ \frac{1}{2(\rho^2 - 1)} - \frac{2(\rho^2 + 1)}{\rho^2 - 1} + 1 \right] \left[ \frac{2\rho^2}{\rho^2 - 1} + \frac{\theta}{2t} \right. \\
 &\quad \left. - \frac{3\theta r}{t^2} \left( \frac{2}{\pi} - 1 \right) \right] \\
 C_i &= \left[ \frac{\rho^2 + 1}{\rho^2 - 1} \right] \left[ \frac{\rho^2 + 1}{\rho^2 - 1} - \frac{1}{2(\rho - 1)} + 1 \right] \\
 &\quad + \left[ \frac{1}{4(\rho - 1)^2} + \frac{1}{2(\rho - 1)} + 1 \right]
 \end{aligned}$$

and

$$\rho = r_o/r_i$$

$$r = \frac{r_o + r_i}{2} = \text{mean tube radius}$$

$$R_o = R + r_o = \text{outside cylinder radius}$$

and

$$p_o = -\frac{\beta_i p_t}{2\gamma_i} \pm \sqrt{\frac{\beta_i^2 p_t^2}{4\gamma_i^2} + \frac{\sigma_y^2}{\gamma_i} - \frac{\alpha_i p_t^2}{\gamma_i}} \quad (16)$$

where

$$\alpha_i = C_i$$

$$\begin{aligned}
 \beta_i &= \left[ \frac{1}{2(\rho - 1)} - \frac{2(\rho^2 + 1)}{\rho^2 - 1} - 1 \right] \left[ \frac{\theta}{2t} - \frac{3\theta r}{t^2} \left( \frac{2}{\pi} - 1 \right) \right] \\
 &\quad + \frac{\rho R_o}{\pi t} \left[ \frac{\rho^2 + 1}{\rho^2 - 1} - \frac{1}{\rho - 1} - 1 \right]
 \end{aligned}$$

$$\begin{aligned}
 \gamma_i &= \left[ \frac{\rho R_o}{\pi t} - \frac{\theta}{2t} + \frac{3\theta r}{t^2} \left( \frac{2}{\pi} - 1 \right) \right]^2 \\
 &\quad + \frac{\rho R_o}{\pi t} \left[ \frac{\theta}{2t} - \frac{3\theta r}{t^2} \left( \frac{2}{\pi} - 1 \right) \right]
 \end{aligned}$$

### Outer Surfaces

For the portion of the tubing on the outside surface of the cylinder

$$\sigma_r = -P_o$$

$$\sigma_\theta = \sigma_{\theta 1} - \sigma_{\theta 2}$$

$$\sigma_{\theta 1} = \frac{2Pt - P_o(\rho^2 + 1)}{\rho^2 - 1}$$

$$\sigma_{\theta 2} = \frac{\rho P_o}{2t} + \frac{3\rho P_o r}{t^2} \left( \frac{2}{\pi} - 1 \right)$$

$$\sigma_x = \frac{Pt}{2(\rho - 1)} - \frac{\rho R_o P_o}{\pi t}$$

For the portion of the tubing on the inside surface of the cylinder

$$\sigma_r = 0$$

$$\sigma_\theta = \sigma_{\theta 1} - \sigma_{\theta 2}$$

$$\sigma_{\theta 1} = \frac{2Pt}{\rho^2 - 1}$$

$$\sigma_{\theta 2} = \frac{\rho P_o}{2t} + \frac{3\rho P_o r}{t^2} \left( \frac{2}{\pi} - 1 \right)$$

$$\sigma_x = \frac{Pt}{2(\rho - 1)} - \frac{\rho R_o P_o}{\pi t}$$

Solving in the same manner as for the inner surface of the tubing results in the following expressions for the maximum allowable  $P_o$

$$P_o = -\frac{B_o P_t}{2A_o} \pm \sqrt{\frac{B_o^2 P_t^2}{4A_o^2} + \frac{\sigma_y^2}{A_o} - \frac{C_o P_t^2}{A_o}} \quad (17)$$

where

$$\begin{aligned}
 A_O &= [\frac{\rho^2 + 1}{\rho^2 - 1} + \frac{\theta}{2t} + \frac{3\theta r}{t^2} (\frac{2}{\pi} - 1)]^2 \\
 &\quad + \frac{\rho R_O}{\pi t} [\frac{\rho R_O}{\pi t} - \frac{\rho^2 + 1}{\rho^2 - 1} - \frac{\theta}{2t} - \frac{3\theta r}{t^2} (\frac{2}{\pi} - 1) - 1] \\
 &\quad - [\frac{\rho^2 + 1}{\rho^2 - 1}] - \frac{\theta}{2t} - \frac{3\theta r}{t^2} (\frac{2}{\pi} - 1) + 1 \\
 B_O &= \frac{\rho R_O}{\pi t} [\frac{2}{\rho^2 - 1} - \frac{1}{\rho - 1}] + [\frac{\rho^2 + 1}{\rho^2 - 1}] [\frac{1}{2(\rho - 1)} - \frac{4}{\rho^2 - 1}] \\
 &\quad + [\frac{1}{2(\rho - 1)} - \frac{4}{\rho^2 - 1}] [\frac{\theta}{2t} + \frac{3\theta r}{t^2} (\frac{2}{\pi} - 1)] \\
 &\quad + \frac{2}{\rho^2 - 1} + \frac{1}{2(\rho - 1)} \\
 C_O &= [\frac{1}{\rho^2 - 1}] [\frac{4}{\rho^2 - 1} - \frac{1}{\rho - 1}] + \frac{1}{4(\rho - 1)^2}
 \end{aligned}$$

and

$$P_O = -\frac{\beta_O}{2\gamma_O} \pm \sqrt{\frac{\beta_O^2 P_t^2}{4\gamma_O^2} + \frac{\sigma_y^2}{\gamma_O} - \frac{\alpha_O P_t^2}{\gamma_O}} \quad (18)$$

where

$$\begin{aligned}
 \alpha_O &= C_O \\
 \beta_O &= [\frac{1}{2(\rho - 1)} - \frac{2}{\rho^2 - 1}] [\frac{\theta}{2t} + \frac{3\theta r}{t^2} (\frac{2}{\pi} - 1)] \\
 &\quad + \frac{\rho R_O}{\pi t} [\frac{2}{\rho^2 - 1} - \frac{1}{\rho - 1}] \\
 \gamma_O &= [\frac{\rho R_O}{\pi t} - \frac{\theta}{2t} - \frac{3\theta r}{t^2} (\frac{2}{\pi} - 1)]^2 \\
 &\quad + \frac{\rho R_O}{\pi t} [\frac{\theta}{2t} + \frac{3\theta r}{t^2} (\frac{2}{\pi} - 1)]
 \end{aligned}$$

and all other terms are as previously defined.

It should be noted that both the external pressure ( $P_o$ ) and the tube pressure ( $P_t$ ) are absolute pressures. Also, the assumption was made that the internal cylinder pressure was zero (as can be seen in Figure I-1). In actual practice the internal cylinder pressure may be considered atmospheric, and the values of  $P_o$  and  $P_t$  may be gage pressures.

For a complete analysis, it is necessary to know the maximum allowable tube pressure. In order to find this pressure, we will again use the von Mises Yield Criterion.

#### Inner Surface

The stresses are the same as those defined previously. Substituting these stresses into the yield criterion and solving for  $P_t$  results in the following equations.

$$P_t = -\frac{B_i P_o}{2C_i} \pm \sqrt{\frac{B_i^2 P_o^2}{4C_i^2} + \frac{\sigma_y^2}{C_i} - \frac{A_i P_o^2}{C_i}} \quad (19)$$

and

$$P_t = -\frac{\beta_i P_o}{2\alpha_i} \pm \sqrt{\frac{\beta_i^2 P_o^2}{4\alpha_i^2} + \frac{\sigma_y^2}{\alpha_i} - \frac{\gamma_i P_o^2}{\alpha_i}} \quad (20)$$

where all terms are the same as those previously defined.

#### Outer Surface

All stresses are the same as those used previously. Solving in the same manner as used above results in the following equations

$$P_t = - \frac{B_o P_o}{2C_o} \pm \sqrt{\frac{B_o^2 P_o^2}{4C_o^2} + \frac{\sigma_y^2}{C_o} - \frac{A_o P_o^2}{C_o}} \quad (21)$$

and

$$P_t = - \frac{\beta_o P_o}{2\alpha_o} \pm \sqrt{\frac{\beta_o^2 P_o^2}{4\alpha_o^2} + \frac{\sigma_y^2}{\alpha_o} - \frac{\gamma_o P_o^2}{\alpha_o}} \quad (22)$$

and all other terms are as defined previously.

To obtain what might be the maximum value of  $P_t$ , differentiate Equations (19) through (22) with respect to  $P_o$ , and set the resulting expressions equal to zero. This results in the following equations for  $P_o$

$$P_o = \frac{\sigma_y}{[\frac{4C_i A_i}{B_i^2} - A_i]^{\frac{1}{2}}} \quad (23)$$

$$P_o = \frac{\sigma_y}{[\frac{4\alpha_i \gamma_i}{\beta_i^2} - \gamma_i]^{\frac{1}{2}}} \quad (24)$$

$$P_o = \frac{\sigma_y}{[\frac{4C_o A_o}{B_o^2} - A_o]^{\frac{1}{2}}} \quad (25)$$

$$P_o = \frac{\sigma_y}{[\frac{4\alpha_o \gamma_o}{\beta_o^2} - \gamma_o]^{\frac{1}{2}}} \quad (26)$$

The maximum allowable tube pressure is obtained by calculating the  $P_o$ 's from Equations (23) through (26) and substituting the values into the corresponding equations for  $P_t$  [i.e., the value for  $P_o$  obtained from Equation (23) is substituted into Equation (19)]. The values obtained in this manner are then compared, and the minimum value of  $P_t$  from the four is used as the maximum allowable tube pressure.

The above method may not yield the maximum value of  $\underline{P_t}$ . This can be quickly checked by taking a value of  $\underline{P_o}$  above, and one below the value of  $\underline{P_o}$  used to determine the maximum allowable tube pressure. These two values are then substituted into the equation that was used to obtain the maximum value of  $\underline{P_t}$ . If either of the resulting values of  $\underline{P_t}$  is greater than the value obtained previously by using Equations (23) through (26), an iteration procedure must be used to find the maximum allowable value of  $\underline{P_t}$ .

The iteration procedure is as follows. The value of  $\underline{P_o}$  is set equal to zero, and this value is substituted into Equations (19) through (22) and the corresponding values of  $\underline{P_t}$  are calculated. A new value of  $\underline{P_o}$  is then selected, and the process is repeated. The iteration is terminated when either a negative tube pressure has been obtained, or when the argument under the square root sign becomes negative (this may not occur at the same value of  $\underline{P_o}$  for each of the equations). Once the iteration has been stopped for one equation, this equation is not used further, but the process is continued using the three remaining equations. The process is halted when the iterations have been stopped for all four equations. The maximum value of  $\underline{P_t}$  obtained for each equation is then found by inspection of the results. The minimum of the four maximums obtained in this manner is then used as the maximum allowable internal tube pressure.

## APPENDIX II

## CONVENTIONAL CYLINDRICAL SHELL ANALYSIS

## A. Buckling

The following equation was given by Timoshenko in reference [14].

$$\begin{aligned} P_{cr} = & \frac{Et}{R} \left[ \frac{1}{n^2 + \frac{1}{2} \left( \frac{\pi R}{L} \right)^2} \right] \left[ \frac{1}{\left( n^2 - \left[ \frac{L}{\pi R} \right]^2 + 1 \right)^2} \right. \\ & \left. + \frac{t^2}{12R^2(1 - \nu^2)} (n^2 + \left[ \frac{\pi R}{L} \right]^2)^2 \right] \end{aligned} \quad (27)$$

This equation is valid for a thin-walled cylinder with closed ends subject to uniform external pressure. The value of n which must be used is the integer value which makes P<sub>cr</sub> a minimum (where P<sub>cr</sub> is the critical pressure for buckling, above this value of pressure the cylinder will buckle).

The value of n can be determined by two different methods. The first is by using the plot given in Figure III-1. The second method is to differentiate the equation for P<sub>cr</sub> with respect to n, and set the resulting equation equal to zero. The quantity n can then be solved for. This procedure results in the following equation

$$\begin{aligned} 0 = & \left( \frac{6}{\mu^6} \right) n^{11} + \left( \frac{28}{\mu^4} \right) n^9 + \left( \frac{52}{\mu^2} \right) n^7 + 48n^5 \\ & + \left( 22\mu^2 - \frac{6\eta}{\mu^2} \right) n^3 + \left( 4\mu^4 - 4\eta \right) n \end{aligned} \quad (28)$$

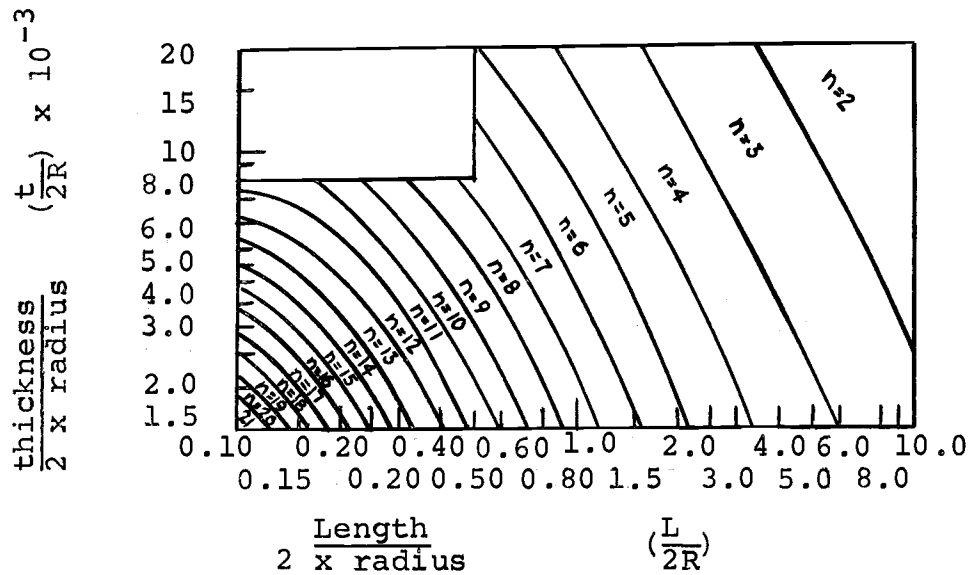


Figure II-1. Plot for determining number of lobes (n).

where

$$\mu = \frac{\pi R}{L}$$

$$\eta = \frac{12R^2(1 - \nu^2)}{t^2}$$

The correct value of  $n$  can be determined by substituting successive values of  $n$  into Equation (28) ( $n$  must be an integer greater than zero). When the sign of the resulting quantity changes, take the value of  $n$  and substitute this value of  $n$  into Equation (27), and calculate the value for  $P_{cr}$ .

### B. Yielding

Assuming the cylinder is thin-walled (as was done for the buckling case) results in the following stresses

$$\sigma_r = 0$$

$$\sigma_\theta = - \frac{P_o R}{t}$$

$$\sigma_x = - \frac{P_o R}{2t}$$

Using the von Mises Yield Criterion and solving for  $P_o$  results in the following equation

$$P_o = \frac{2t\sigma_y}{\sqrt{3} R} \quad (29)$$

## APPENDIX III

COMPARISON OF CONVENTIONAL AND PRESTRESSED  
CYLINDRICAL SHELLS

It was decided that the best way of comparing conventional and prestressed cylinders was on the basis of total weight. This was done by assuming the two types of cylinders (conventional and prestressed) were of the same length, mean radius, and weight. By making these assumptions an equivalent wall thickness for the conventional cylinder can be computed, and from this the comparisons can be made.

## A. Prestressed Cylinder

$$\text{Number of Coils} = N = \frac{L}{2r_o}$$

$$\text{Cross-sectional Area of Tubing} = A = 2\pi r_i t$$

$$\text{Length of Single Coil} = C = 2\pi R$$

$$\text{Total Volume of Material} = V = NCA = \frac{2\pi^2 L R t r_i}{r_o}$$

Since the densities of the two cylinders are the same (they are assumed to be constructed from the same material), only the volumes need to be compared since

$$\text{Weight} = \text{Density} \times \text{Volume}$$

## B. Conventional Cylinder

$$V = 2\pi R t' L$$

where

$t'$  = wall thickness of conventional cylinder

Equating the two volume terms to obtain the desired conventional cylinder wall thickness ( $\underline{t'}$ ) results in

$$t' = \frac{\pi r_i t}{r_o} = \frac{\pi t}{\rho} \quad (30)$$

where

$t$  = Tube Wall Thickness

$$\rho = \frac{r_o}{r_i}$$

Table III-1. Data for tube wall thickness of 0.05 inches.

R/r	R	Outside Tube Radius ( $r_o$ )	$P_o$ Conventional	$P_o$ Prestressed
142.9	50	0.375	12.62	7.578
105.3	50	0.500	13.62	5.584
69.0	50	0.750	14.68	3.641
51.3	50	1.00	15.23	2.688
16.8	50	3.00	16.38	0.8201
10.1	50	5.00	16.62	0.4559
7.2	50	7.00	16.72	0.3029
5.6	50	9.00	16.78	0.1482
4.6	50	11.00	16.82	0.1132
285.7	100	0.375	1.982	3.820
210.5	100	0.500	2.398	2.821
137.9	100	0.750	2.582	1.849
102.6	100	1.00	2.679	1.371
33.6	100	3.00	2.879	0.4345
20.1	100	5.00	2.921	0.2503
14.3	100	7.00	2.938	0.1720
11.1	100	9.00	2.948	0.1289
9.1	100	11.00	2.955	0.1016
428.6	150	0.375	0.7418	2.554
315.8	150	0.500	0.8054	1.888
206.9	150	0.750	0.8729	1.239
153.8	150	1.00	0.9820	0.9205
50.4	150	3.00	1.327	0.2954
30.2	150	5.00	1.343	0.1723
21.5	150	7.00	1.349	0.1199
16.7	150	9.00	1.353	0.0909
13.7	150	11.00	1.355	0.0725
571.4	200	0.375	0.3633	1.918
421.1	200	0.500	0.3941	1.418
275.9	200	0.750	0.4268	0.9316
205.1	200	1.00	0.4439	0.6928
67.2	200	3.00	0.6368	0.2238
40.2	200	5.00	0.6443	0.1314
28.7	200	7.00	0.6476	0.0919
22.3	200	9.00	0.6494	0.0701
18.2	200	11.00	0.6505	0.0563

Table III-2. Data for tube wall thickness of 0.30 inches.

R/r	R	Outside Tube Radius ( $r_o$ )	$P_o$ Conventional	$P_o$ Prestressed
83.3	50	0.750	391.8	139.2
58.8	50	1.00	457.1	108.8
17.5	50	3.00	576.3	30.88
10.3	50	5.00	613.8	16.87
7.3	50	7.00	625.0	10.99
5.6	50	9.00	631.2	7.952
4.6	50	11.00	635.2	6.076
166.7	100	0.750	70.72	60.28
117.6	100	1.00	113.3	55.47
35.1	100	3.00	197.8	16.07
20.6	100	5.00	219.1	9.143
14.6	100	7.00	228.7	6.252
11.3	100	9.00	234.2	4.671
9.2	100	11.00	237.7	3.678
250.0	150	0.750	25.52	40.36
176.5	150	1.00	40.43	37.22
52.6	150	3.00	70.72	10.94
30.9	150	5.00	78.36	6.300
21.9	150	7.00	132.2	4.360
16.9	150	9.00	134.3	3.296
13.8	150	11.00	135.6	2.624
333.3	200	0.750	13.62	30.25
235.3	200	1.00	18.88	27.52
70.2	200	3.00	35.79	8.288
41.2	200	5.00	39.12	4.805
29.2	200	7.00	42.64	3.346
22.6	200	9.00	43.55	2.544
18.4	200	11.00	44.14	2.038

Table III-3. Data for tube wall thickness of 0.55 inches.

R/r	r	Outside Tube Radius ( $r_o$ )	$P_o$ Conventional	$P_o$ Prestressed
105.3	50	0.750	240.7	251.1
69.0	50	1.00	538.7	310.9
18.3	50	3.00	977.6	107.9
10.6	50	5.00	1065.	58.10
7.4	50	7.00	1103.	38.05
5.7	50	9.00	1124.	27.39
4.7	50	11.00	1137.	20.85
210.5	100	0.750	44.63	125.4
137.9	100	1.00	162.0	156.4
36.7	100	3.00	488.8	57.18
21.2	100	5.00	532.7	31.89
14.9	100	7.00	551.5	21.60
11.5	100	9.00	562.0	16.05
9.3	100	11.00	568.6	12.59
315.8	150	0.750	16.19	83.46
206.9	150	1.00	57.88	104.5
55.0	150	3.00	253.0	38.88
31.7	150	5.00	355.1	21.96
22.3	150	7.00	367.7	14.81
17.2	150	9.00	374.7	11.16
14.0	150	11.00	379.1	8.875
421.1	200	0.750	7.661	62.53
275.9	200	1.00	27.42	78.48
73.4	200	3.00	130.7	29.45
42.3	200	5.00	158.0	16.43
29.7	200	7.00	170.8	11.37
22.9	200	9.00	178.3	8.624
18.6	200	11.00	183.2	6.896